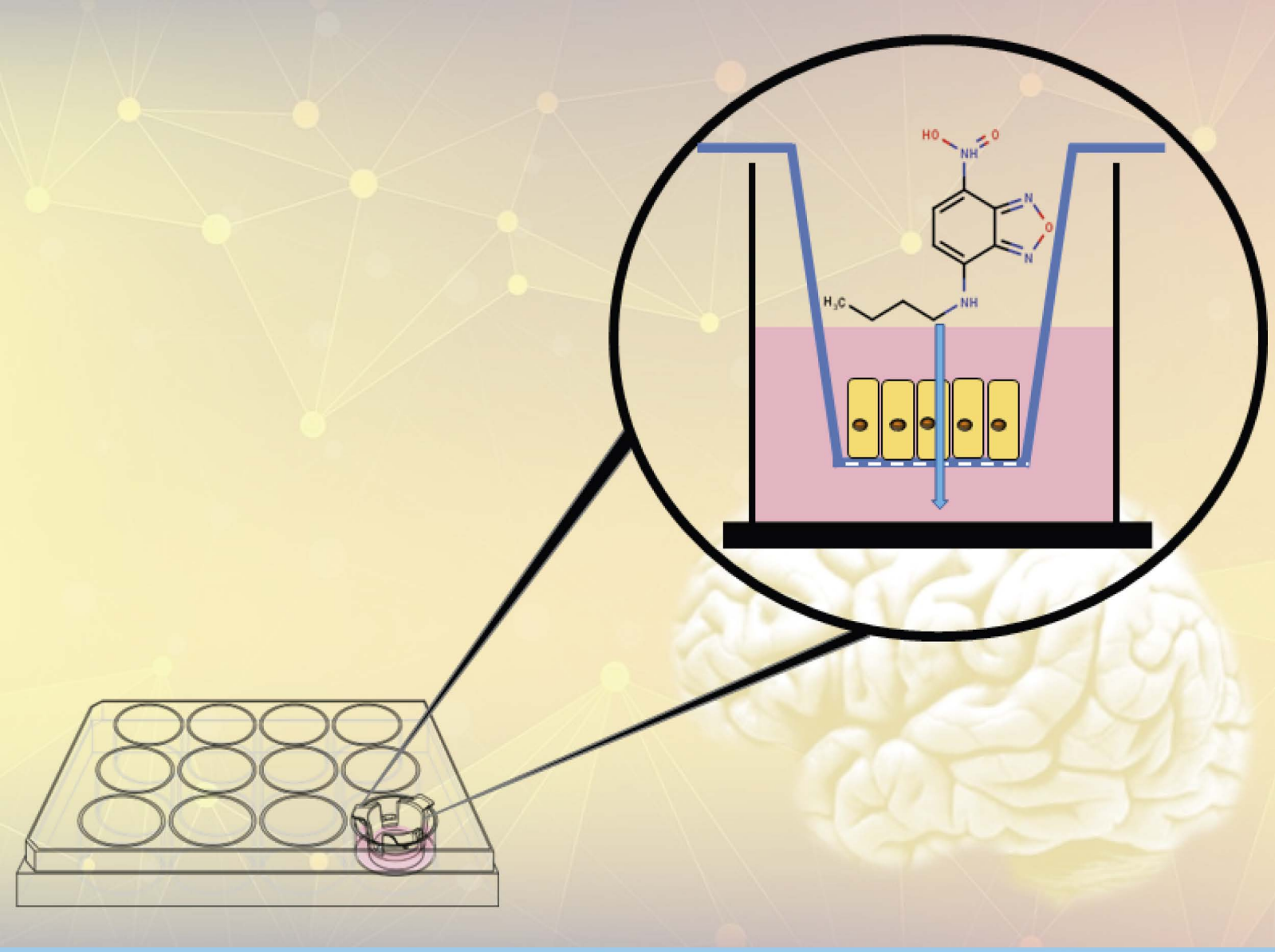

Cristiana Lages Pires

Permeability through Caco-2 cell monolayers as a model for BBB: implementation and preliminary evaluation using model compounds

Mestrado em Química Medicinal

Departamento de Química

FCTUC

Fevereiro 2018

· U C ·

UNIVERSIDADE DE COIMBRA

Cristiana Lages Pires

Permeability through Caco-2 cell monolayers as a model for BBB: implementation and preliminary evaluation using model compounds

Dissertação apresentada para provas de Mestrado em Química Medicinal

Orientador: Professora Doutora Maria João Moreno

Fevereiro 2018

Universidade de Coimbra

Agradecimentos

Gostaria de aproveitar esta oportunidade para expressar a minha mais profunda gratidão às pessoas que me apoiaram durante a preparação desta tese.

Agradeço em particular à professora Maria João Moreno, pelo seu contínuo encorajamento, disponibilidade, amizade, apoio financeiro, profissionalismo e especialmente pela orientação científica. Foi incansável, sempre com resposta pronta a todas as minhas dúvidas.

Agradeço aos meus colegas de laboratório, do Grupo de Química Biológica: Zaida, Jaime, Hugo, Filipe e Raquel, tanto pelas discussões científicas como pelas conversas mais descontraídas tornando os meus dias no laboratório mais agradáveis.

Agradeço igualmente aos meus colegas dos laboratórios de cultura celular: Hélder Soares, Catarina Lobo, Ana Lúcia e Inês Lamego pela sua ajuda e ensinamentos. Á Catarina Almeida, do grupo de Biomaterials and Stem Cell-Based Therapeutics do Biocant, agradeço por me ter acolhido no seu laboratório, pela sua disponibilidade, amabilidade e conhecimento transmitido.

Às minhas amigas, Helena, Andreia e Bia pela sua amizade, companheirismo, preocupação e incentivo nos momentos de maior desânimo.

Aos meus pais e irmã, pelo seu amor, carinho e inspiração.

Ao David, pelo seu carinho, encorajamento, paciência e compreensão nas ausências dedicadas à investigação.

Muito obrigada!

Table of Contents

Abbreviations

AT – atenolol

BBB – blood-brain barrier

bFGF – basic fibroblast growth factor

BSA – bovine serum albumin

CNS – central nervous system

Caco-2 – colon adenocarcinoma cell line

DMEM – dulbecco´s modified eagle´s medium

DMSO – dimethyl sulfoxide

ECs – endothelial cells

EGM-2 –endothelial growth medium

EBM-2–endothelial basal medium

FBS – fetal bovine serum

HBSS – hank's balanced salt solution

LY – lucifer yellow

HPLC– high performance liquid chromatography

NBD-C4 – (7- nitrobenz-2-oxa-1,3-diazol-4-yl) aminobutanoyl

NEAA – non-essencial amino acids

P_{app} – apparent permeability coefficient

P_c – cellular permeability

PBS – Phosphate-buffered saline

P_e – endothelial permeability

P_f – filter permeability

P-gp – P-glycoprotein

QSPR – quantitative structure property relationships

TEER – transephitelial resistance

ZO-1 – zonula occludens protein-1

VEGF – vascular endothelial growth factor

List of figures

List of Tables

Resumo

Nas fases iniciais do desenvolvimento de fármacos, a capacidade que o composto tem de atravessar as membranas biológicas é um factor determinante na selecção de candidatos a fármaco. Este processo é particularmente relevante no caso de fármacos administrados por via oral, uma vez que estes têm de ser absorvidos ao nível do tracto gastrointestinal para atingirem o alvo de interesse. Compostos direccionados ao sistema nervoso central tem adicionalmente de atravessar a barreira hematoencefálica (BHE), que por sua vez impõe mais restrições às propriedades do fármaco.

De uma forma geral, os fármacos permeiam as membranas celulares por processos passivos, uma vez que não são reconhecidos por transportadores específicos. Adicionalmente, os fármacos podem ser substratos de transportadores de efluxo, tais como a glicoproteína-P, o que limita a sua permeação passiva em direcção ao tecido/receptor alvo.

O uso de modelos *in vitro* que mimetizam as membranas biológicas é de extrema importância para avaliar a biodisponibilidade de um fármaco. A linha celular de adenocarcinoma do cólon humano (Caco-2) é um modelo *in vitro* bem caracterizado do epitélio intestinal, usado para prever a permeabilidade intestinal de fármacos e a sua absorção oral em humanos. Este modelo tem sido extensivamente usado pela comunidade científica dando origem a uma grande quantidade de dados. Infelizmente, a discrepância entre os coeficientes de permeabilidade reportados por diferentes grupos de investigação é enorme, muitas vezes diferindo em várias ordens de grandeza. Isto impede a sua utilização para a obtenção de relações quantitativas estrutura-propriedade (QSRPs) que possam ser aplicadas para prever a biodisponibilidade de fármacos nas células e tecidos. Estas discrepâncias podem surgir de várias fontes, nomeadamente do número de passagem das células ou das condições experimentas usadas no ensaio de permeabilidade (particularmente a composição do meio de transporte).

Neste trabalho, implementaram-se ensaios de permeabilidade *in vitro* usando o modelo Caco-2 para vários compostos. O efeito da presença de albumina nos compartimentos dador/aceitante foi quantitativamente avaliada e racionalizada em termos da fracção de composto livre. Os coeficientes de permeabilidade aparente foram interpretados tendo em conta a interacção do composto com os componentes do meio de transporte bem como com as membranas das células, usando um modelo cinético desenvolvido no grupo.

O objectivo último deste trabalho é o estabelecimento de QSRPs com vista a entender e prever a velocidade de permeação através de monocamadas de células, tais com a

BHE. Com este objectivo, foram realizados ensaios de permeabilidade em células endoteliais obtidas a partir de células estaminais hematopoéticas. A comparação entre os resultados obtidos nos dois modelos celulares permitirá uma melhor caracterização das propriedades das diferentes membranas biológicas, e uma optimização das propriedades do fármaco tendo em conta o seu tecido alvo.

Abstract

In early stages of drug discovery, the capacity of a compound to cross biological membranes is a determining factor in the selection of drug candidates. This is very important in the case of orally administered drugs once they must be absorbed at the gastrointestinal tract in order to reach the target of interest. Compounds targeted to the central nervous system have also to overcome the blood-brain barrier (BBB), which imposes even more constraints on the drug properties.

In general, passive permeation is the major route for the intake of drugs across cell membranes, as they are usually not recognized by specific transporters. Additionally, drugs may be substrates of active efflux pumps such as P-glycoprotein, which further limits their effective permeation towards the target tissue/receptor.

The use of *in vitro* models to mimic biological barriers is of extreme importance to evaluate drug's bioavailability. The human colon carcinoma cell line Caco-2 is a well characterized *in vitro* model of the intestinal epithelium for prediction of intestinal drug permeability and oral drug absorption in humans. This model has been thoroughly used by the scientific community and has delivered a large amount of data. Unfortunately, the discrepancy between the permeability coefficients reported by different research groups is very large, often differing by several orders of magnitude. This precludes the use of this information to obtain Quantitative Structure Property Relationships (QSPR) that may be reliably applied to predict drug's bioavailability in cells and tissues. Those discrepancies may come from several sources, namely the cell passage number or the experimental conditions used in the permeability assay (particularly the composition of the transport media).

In this work we implement *in vitro* permeability assays using the Caco-2 cell model, for several model drugs. The effect of the presence of serum albumin in the donor/receiver compartment was quantitatively evaluated and rationalized in terms of the free fraction of drug. The apparent permeability coefficient was interpreted taking into account the drug's interaction with components of the transport media as well as with the cell membranes, using the kinetic model recently developed in our group.

The ultimate goal of this study is the establishment of QSPR, with a view to understand and predict the rate of drug permeation through cell monolayers such as the BBB. With this objective, permeability assays using endothelial cells obtained from Hematopoietic Stem Cells, have been undertaken. Comparison between the results obtained with the two distinct cell models allows a better characterization of the properties of the different biological barriers, and an optimization of the drug's properties depending on their target tissue.

Chapter 1

Introduction

1.1 In search for predictive screening models of drug permeability

In the drug discovery process, the screening of large compound libraries using high-throughput screening methods facilitates the rapid identification of pharmacologically active compounds. Although this process has proven to be successful in terms of generating lead compounds with high affinity for the selected target (1), the development of potential drug candidates is hampered due to unfavorable pharmacokinetics properties (2). The existence of activity/interaction does not guarantee *in vivo* efficacy, therefore the compounds identified by high-throughput screening should be well characterized in terms of permeability, metabolism and toxicity.

The major causes of drug failure in clinical trials are unexpected toxicity and lack of efficacy (3, 4). In most recent analysis, the cost of getting a drug to market is approaching US$1.4 billion and the cost of advancing a compound to phase I trials can reach up to US$430 million (5). Thus, to reduce drug attrition in late clinical development it is of the highest importance the early recognition of problems that would make a compound unlikely to succeed in development. The extent of the drug penetration through the biological barriers such as the cell membrane, intestinal wall or blood-brain barrier (BBB) is determinant for both efficacy and toxicity profile in clinical trials (4). The development of drugs targeting the central nervous system (CNS) or for oral administration requires precise knowledge of the drug's permeation through biological barriers. Orally administered drugs must be absorbed at the gastrointestinal tract (GI) in order to reach the target of interest. Compounds targeting the CNS have additionally to overcome the BBB, which imposes even more constraints on the drug properties. Therefore, evaluation of the bioavailability (ability to cross biological barriers) of drug candidates should be addressed as early as possible, in preclinical candidate selection stages. This will guarantee that development can focus resources on compounds more-likely-to-succeed as drug candidates.

There are various routes by which a drug can cross epithelial and endothelial barriers (**Figure 1**). Passive diffusion is driven by a concentration gradient and may occur through transcellular (across the cells) or paracellular (through the tight junctions between the cells) pathways, depending on drug´s lipophilicity. Compounds may in addition or alternatively be recognized by transport proteins and permeation occurs through carrier-mediated transport via active processes or by facilitated diffusion. Influx

transporters contribute significantly to the uptake of the drug into the cell contrarily to efflux transporters that transport the drug out of the cell, such as P-glycoprotein (P-gp). It is thus advisable to identify whether or not the drug candidate is a substrate of efflux transporters in the early phase of drug discovery. Finally, receptor-mediated transcytosis could also be a possible route. In general, passive permeation is the major route for the intake of drugs across cell membranes, as they are usually not recognized by specific transporters (6).

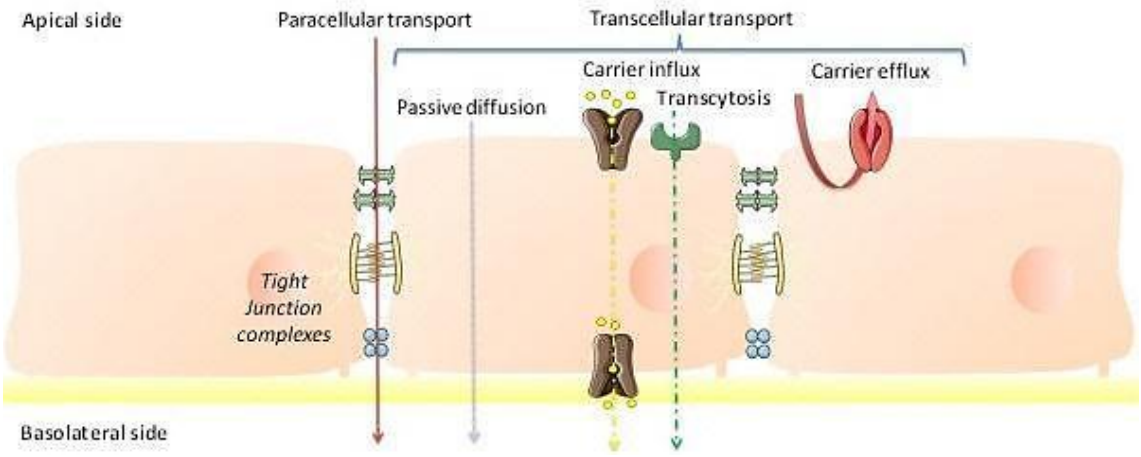

Figure 1 - Pathways for drug transport across biological barriers. The endothelial and epithelial cells layers form a selective barrier which drugs may overcome by more than one mechanism. In case of endothelial cells, the apical side represents the blood and the basolateral side the CNS. The apical and basolateral sides of epithelial cells corresponds to intestinal lumen and blood, respectively. Adapted from (7).

As the majority of drugs are administered via the oral route, the extent of intestinal absorption is one of the key properties for drugs. If a drug with high-affinity to its intended target has poor intestinal permeability, is unlikely to demonstrate the desired efficacy. The task of predicting the intestinal mucosa permeability of new compounds during absorption is essential for successful oral drug therapy (8).

Neuroactive drugs have the additional complexity/difficulty of achieving sufficient BBB penetration to elicit a response. Permeability through the BBB, to reach a target in the CNS, is restricted by specialized tight junctions connecting the endothelial cells of the brain capillaries, which create a selective barrier between the brain and the rest of the body. Additionally, the membrane of BBB endothelial cells have high levels of efflux transporters, specially P-gp (9, 10). Those proteins actively transport the drug from the membrane into the blood, further limiting the effective permeability towards the target/receptor and therefore reducing drug's efficacy. The low permeability of the BBB is crucial to protect the brain from the eventually toxic molecules present in the blood

(10). However, this imposes important constraints in the design of drugs targeted for CNS disorders, and should be addressed early in the drug discovery process.

By using a model system that properly mimic the *in vivo* features of biological barriers it´s possible to create adequate screening systems that can be used to predict or asses the bioavailability of a compound at their active site. Facing the extraordinary cost of new drug development it would be highly desirable to have effective, low cost and high-throughput predictive screening models of drug permeability or absorption to gain early insight into the potential of lead compounds before they failed in late-stage clinical trials (11). Correspondingly, the permeation predictions of the promising drug candidate will allow appropriate optimization of permeability properties at the earliest stages in drug discovery. A drug candidate without effective permeation could be structurally optimized to increase intrinsic permeability improving the probability of success in clinical trials.

1.2 Models to predict drug´s permeability

In an attempt to design and select drug candidates which cross epithelial and endothelial barriers it is important to predict drug´s permeability and characterize the processes involved in permeation. Screening assays for the prediction of drug´s permeability are becoming fundamental as part of the drug development process. As a result, several models have been developed to mimic the absorptive barrier of the intestine and the BBB. These models are useful tools for permeability screening purposes. The existent models range in complexity, comprising *in vivo*, *in situ* and *in vitro* experimental methods and *in silico* computational methods.
Currently used models for the assessment of drug permeability include *in vivo* whole animal studies, Using chamber, *in-situ* perfused tissue preparations, cell-based systems and artificial lipid membranes (8, 12, 13).

In vivo models are of great interest because they are the only ones taking into account the dynamic components of the blood circulation and tissue layers that may have impact on bioavailability (12). However, due to the utilization of different species, the information obtained from experimental animal models cannot always be transposed to the human. Also, those *in vivo* experiments require sophisticated equipment, technical expertise and tend to be time consuming, invasive and low throughput (8). For these

reasons, but particularly because financial and ethical concerns about the animal well care, in vivo studies are unsuitable for use during early stages of drug discovery and development (12). The present need for more rapid, economical and low time consumption methodologies for prescreening is continuously pushing researchers to use easy and fast *in vitro* experimental models.

Attractive alternative models for determining the permeability of potential drug candidates include those based on artificial membranes, such as the Parallel Artificial Membrane Permeability Assay (PAMPA) and *in vitro* cell based assays.

Although *in vitro* systems lack the complexity and variability found in *in vivo* models, cell based models have been designed with sufficient relevant features including high similarity in cell morphology compared to the native tissue and expression of various drug transport systems and metabolic enzymes to resemble the *in vivo* like situation.

The development of cell culture inserts with porous membranes in a vertical side by side diffusion system (e.g. Transwell) has led to major improvements in modeling biological barriers *in vitro*. When grown on culture inserts, confluent monolayers exhibiting good barrier properties are formed. The configuration of these systems is designed to allow access to both apical and basolateral compartments, which permits permeability measurement through the cell monolayer in the Apical to Basolateral (A-B) and Basolateral to Apical (B-A) directions (11).

Although most cellular models are simple monocellular layers, refinements are possible in order to mimic as closely as possible biological barriers, like incorporating more than one type of cells, co-cultures and advanced dynamic systems (14).

To date, numerous cell culture models are employed as well-established models of intestinal and BBB barriers for permeability assessment studies of various drug compounds (11, 15).

More than ever, due to the large number of compounds that need to be screened, it is vital to have an easy and fast *in vitro* model for permeability screening assessment in early stages of drug development. *In vitro* cell models are easy to manipulate, reproducible and cost-effective methods. Most of these tools can be automated for high throughput drug permeability screening applications. The popularity of cell lines models can probably be explained by the ease which new information is derived from them (16). Despite the widespread use of *in vitro* cell models, validation of the extrapolation of *in vitro* findings *to in vivo* human conditions is necessary to further use in future drug discovery optimization and clinical development. Locking from the other side of the problem, *in vitro* cell models are complex systems where the observed drug permeability may be affected by a large number of factors. Due to this complexity, data

from *in vitro* cell models cannot easily be used to establish quantitative rules to allow the prediction of the permeability for new drugs.
When the aim is to identify the mechanism of permeation and gain predictive power, simpler model systems are of great interest. Liposome based model systems are particularly useful for this purpose due to their similarity to the biological barrier and to the possibility of incorporation of membrane transporters (17).

The application of computational (*in silico*) methods to predict drug permeability is currently another area of intense investigation. The major interest of i*n silico* modeling systems is its potential to accelerate drug discovery by testing a large number of virtual drugs to predict their efficacy and bioavailability. This allows for rapid and inexpensive screening of novel leads giving a preliminary assessment of their efficacy. A major advantage of those methods is that the molecules tested are only virtual. In this way, their properties may be accessed without the costs involved in their synthesis and purification. This makes them a particularly important tool in the early stages of drug discovery (18). There are several approaches to characterize and predict drug-target interactions, for example docking methods (19).
Several efforts to develop computational methods to gain mechanistic insight in permeability processes have also been undertaken (20). For example, a computational mechanistic model of passive permeability profile of a range of compounds through a tight endothelium has been developed in our research group (21).
However, even with latest advances, *in silico* methods are still not able to replace *in vitro* and *in vivo* approaches. Even though they are faster and less expensive, cell-based assays should be used to confirm *in silico* predictions and in lead optimization (22).

1.2.1 Epithelial *in vitro* models

The permeation of drugs across the intestinal epithelial barrier is a major determinant of drug absorption and thus *in vivo* bioavailability. The single layer of epithelial cells in the intestine is the rate-limiting barrier for the uptake of compounds between the lumen and the systemic circulation. Hence, *in vitro* methods based on epithelial monolayers have been chosen over the years as a primary permeability screening tool of the intestinal drug absorption. Several cell lines are in use for modelling intestinal

absorption including human colonic adenocarcinoma cell lines, Caco-2, T84 and cell lines from animals such MDCK (Madin Darby canine kidney) and 2/4/A1(rat) (22) (16).

In particular, the Caco-2 system has emerged as one of the standard *in vitro* tools for intestinal absorption studies. It is probably the most extensively characterized and the most widely used cell-based intestinal model to screen for oral absorption potential in drug discovery (12)

The Caco-2 cell line was originally isolated from a human colon adenocarcinoma, derived from a 72-year-old Caucasian male in the late 1980s (23). Caco-2 cells undergo spontaneous differentiation into cells resembling enterocytes of the small intestine. At confluence they form a polarized monolayer of columnar epithetlial cells displaying brush border microvilli regions in the apical membrane and tight junctions between the cells. Caco-2 cells also express many of the active transporters systems that mediate the uptake or efflux of drugs and enzymes present in the walls of the human small intestine (24). Typically, Caco-2 cells are cultured for 21 days on porous filter supports of a Transwell system to ensure formation of a well-differentiated confluent epithelial cell monolayer (25) (**Figure 2**). A brief summary of the Caco-2 assay procedure is provided in the materials and methods section.

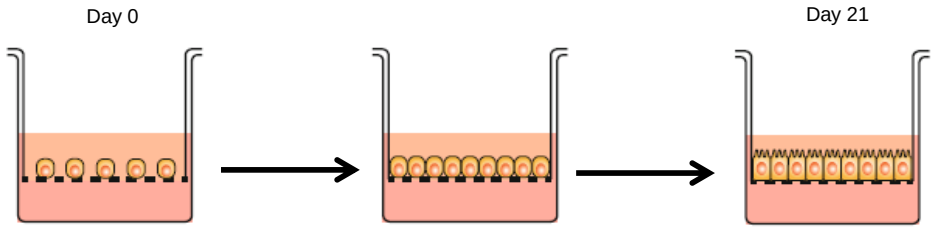

Figure 2 – Schematic representation of the establishment of the *in vitro* Caco-2 model. The Caco-2 cells grown on porous polycarbonate culture insert and after the cells reach confluence (*middle*) they start to differentiate spontaneously. After a culture period of 21 days the cells will from confluent monolayers of well-differentiated enterocyte like cells with an apical brush border with microvilli and tight junctions between adjacent cells. Adapted from (26).

The drug permeability through Caco-2 monolayers is therefore expected to correlate well with that of the intestinal membrane *in vivo* given the many primary-like qualities of enterocytes exhibited by Caco-2 cells. Artursson and Karlsson found a good correlation between the *in vitro* Caco-2 permeability and absorption at the human jejunum for a

series of orally administered drugs which permeate by passive mechanisms (27). In the same study, the drugs with different physicochemical characteristics were categorized with complete, moderate and low absorption in humans with respect to their passive permeability across the Caco-2 cell monolayer. Thus, the *in vitro* permeability across Caco-2 cells monolayers can be used routinely to evaluate the *in vivo* absorption in humans for new compounds.

There are several published reports of successful applications of the Caco-2 system for the prediction of absorption in the intestine. The influence of efflux systems, such as P gp on intestinal drug transport has been studied in this cell line. (28, 29) The common approach involves bidirectional transport of compound in Caco-2 cell using a specific inhibitor and/or specific substrate of the efflux pump.

In addition, the use of the Caco-2 cell assay facilitates the identification of drugs with potential absorption problems and possibly also to select drugs with optimal passive absorption characteristics. The Caco-2 assay is well characterized, easily maintained and manipulated, requires only small quantities of compounds and exhibit adequate predictability of absorption potential in humans (30).

The use of robotics and multi-wells plates enhance the throughput of Caco-2 assays generating automated procedures for screening of drug transport through Caco-2 monolayers. Recently, modified culture protocols that speed up the differentiation process to 3- to 7-day of culture have been published (31). However, characterization of the cell monolayer on the accelerated protocols is still required in order to define the differences as compared to the conventional model.

Genetically engineered Caco-2 cell lines and co-cultures comprising different cells presents in the intestinal epithelium have been proposed to more closely mimic at a cellular level the intestinal epithelium (32). Nevertheless, the use of the Caco-2 model prevails as a screening tool for the assessment of drug permeability and absorption.

1.2.2 BBB *in vitro* models

The BBB is formed by brain endothelial cells (ECs) that constitute the wall of the cerebral capillaries, creating an interface between the blood and the brain. The cerebral capillary ECs are highly connected by adherens and tight junctions (TJs) forming a physical barrier that restrict the entry of most hydrophilic compounds intro the brain (9, 33). Brain capillary ECs are 50-100 times tighter than peripheral ECs (34).

The TJs contribute to this tightness BBB, causing a major restriction in the paracellular pathway of hydrophilic solutes. In addition to ECs, the BBB is composed by pericytes, astrocytes, microglia, and the basement membrane. Together all these cellular components form the neurovascular unit and are fundamental contributors of the BBB integrity (35). The barrier function of brain capillaries is primarily due to the presence of junctional complexes between adjacent endothelial cells and to a high expression pattern of different membrane efflux transporters, namely P-gp, present in the apical surface of the capillary ECs (9).

BBB represents the principal route for the entry of most solutes into the CNS as well as the major obstacle to the development of novel neuropharmaceuticals. For assessing BBB permeability, the development of a functional and well-characterized *in vitro* BBB model is of the greatest importance. *In vitro* BBB models can provide a valuable tool for studying BBB permeability and the transport of drugs to the brain and thus for prediction of the pharmacological activity of the brain targeted drugs before *in* vivo studies (10). Currently, a standard *in vitro* BBB cell culture model that can fully replicate the *in vivo* conditions is not yet available. The research community recognizes that reproducing the physiology and functional properties of the BBB *in vitro* is a challenging work (36). Nevertheless, there are major requirements that an ideal *in vitro* BBB model should resemble. According to Gumbleton and Audus, this includes. low permeability, endothelial-like morphology, expression of functional transporters, such as P-gp, and easy to implement (37).

The first human BBB models were generated 10 years ago from primary human brain ECs and immortalized human cells (38). However ethical limitations in obtaining human tissue and loss of human brain EC phenotype during cell culture, limits their general use. Recently, new human BBB models based on brain ECs derived from human stem cells have been developed (15, 39). Human brain ECs have been differentiated from pluripotent (induced pluripotent and embryonic stem cells) or multipotent stem cells (e.g. hematopoietic progenitor. These stem cells have the capacity to differentiate into brain ECs that can proliferate *in vitro* and thus, can be a promising basis in the generation of *in vitro* human BBB models (39). To better mimic the anatomic structure of the *in vivo* BBB, the induction of BBB properties are established by co-culture of ECs with BBB-inducing cells such as glial cells, astrocytes and pericytes (40, 41). Current co-culture models of the BBB are based on the Transwell systems. Hence, the ECs are cultured in the Transwell insert and the BBB-inducing cell line is grown either on the underside of the Transwell insert or at the bottom of the well plate. However, given the

recent development, these models have not yet been extensively characterized. The human stem cell models are presently being characterized regarding BBB features as well as validating for the reproducibility predictability and ‘‘ease of culture”. The stem cell-derived BBB models present great opportunities as a screening tool for CNS-drug permeability studies.

Recently, a general and relatively easy method to generate a human BBB model using cord blood-derived hematopoietic stem cells or $CD34^+$, have been reported (42). $CD34^+$ which can be obtained non-invasively, were initially differentiated into endothelial cells (ECs) and cultured on the surface of Transwell inserts. Bovine brain pericytes were cultured in the lower chamber of the culture plate. After 6 days of co-culture, the BBB phenotype is induced in the ECs (**Figure 3**). This model is very reproducible, stable and has shown a correlation with *in vivo* human data. Detailed procedure is provided in section materials and methods.

Despite the clear advancement in BBB modeling attempts have been made to develop more sophisticated dynamic (flow-based) co-culture BBB models (14). For routine use, the establishment and maintenance of a co-culture system is very expensive and labor intensive. Alternatively, simpler *in vitro* models for the BBB that does not use cerebral cell lines, and that show some, but not all, BBB features could also been employed. Most recently native MDCK-MDR1 and Caco-2 epithelial cell monolayers were used to predict brain penetration (43-46).

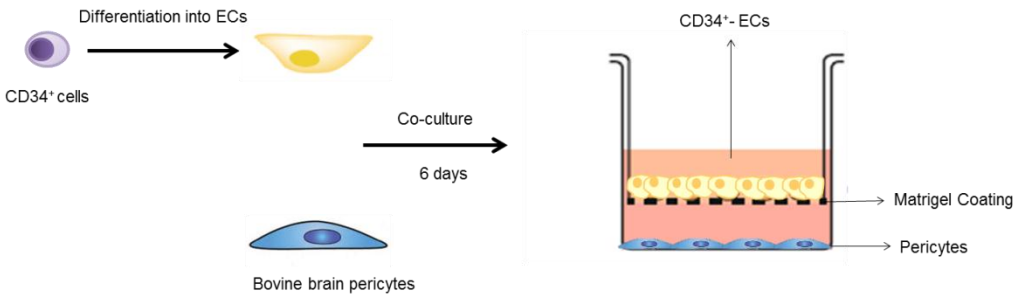

Figure 3 - **In vitro human BBB model derived from stem cells and the protocol for setting it up** .ECs were derived from cord blood-derived $CD34^+$ stem cells. The $CD34^+$ -ECs were co-culture with bovine brain pericytes in a Transwell system for 6 days: ECs were grown on filter inserts coated with Matrigel together with pericytes at the bottom of culture plates.

1.3 Evaluation of structure and function of an *in vitro* barrier model

To perform reliable *in vitro* experiments, a routine characterization of the properties and quality control of the endothelial or epithelial monolayers should be carrying out. Several parameters can be used to evaluate the properties of *in vitro* barrier model including cell morphology, TEER and paracellular permeability.

1.3.1 Morphology

When establishing the technique for growing cells on filter supports, visualization is an important tool to control cells morphology, and verify the monolayer homogeneity and tightness (25). Imufluorescence methods combined with confocal microscopy may be used for this propose. Usually, cytoskeleton, cell nuclei and tight junctions are labeled for visualization. General fluorescent marker, such as nuclear stains and rhodamine-phalloidin (to visualize actin) is sufficient to evaluate if a single layer of cells is present. Immunohistochemical staining of the tight-junction protein zonula occludens 1 (ZO-1) can be used to evaluate the localization of the tight junction.

1.3.2 Properties

Transepithelial/Transendothelial electric resistance (TEER)

As a quality control, the integrity of each epithelial or endothelial monolayer should be verified by measuring the TEER. Electrical resistance measurements are carried out by using a voltmeter equipped with electrodes that are placed in both the lower and upper compartments of the Transwell insert (**Figure 4**). TEER is a measure of the resistance to small ions flux and reflects the integrity of the cell monolayer and the presence of tight junctions. The resistance is routinely measured in the transport medium, before and after the transport experiment. First, to ensure integrity at the time of the experiment, and after, to provide evidence of an eventual toxic effect by the compound studied on monolayer integrity (23).

It is important to point out that TEER is dependent on the type of insert, cell passage number temperature and measuring equipment (47, 48). TEER values are calculated multiplying the resistance value obtained (after subtraction of the resistance value obtained with cell-free filters) by the surface area of the membrane insert to obtain TEER expressed as Ω.cm2. Values above 1000 Ω.cm2 indicate high resistance. Low TEER values are usually indicative of leaky monolayers or holes in monolayers.
TEER values ranging from 62 to 1290 Ω.cm2 have been reported for Caco-2 monolayers (16).

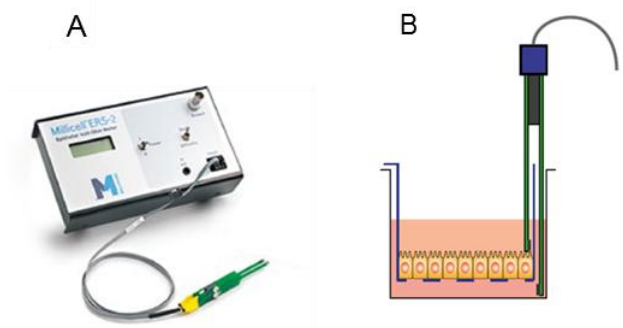

Figure 4 – Setup for TEER measurement. A) Representation of a Millicell ERS-2 voltmeter with a chopstick electrode pair. B) The electrode is placed in the insert, with the shorter tip of the electrode in contact with the cell monolayer while the longer tip touch the bottom of the culture well plate. Adapted from (26)

Permeability to paracellular markers

A more reliable method to assess monolayer integrity is to perform a transport experiment with a hydrophilic marker molecule that is passively transported by the paracellular route across the monolayer. Most common paracellular markers used are radiolabelled mannitol or inulin, or fluorescent compounds such as lucifer yellow (LY) and sodium fluorescein. Such molecules can be used to get information about the integrity of the cell monolayer and/or leakiness of the TJs. Low paracellular permeability is an indication of the presence and integrity of TJ. For example, the permeability values for [^{14}C] mannitol in Caco-2 monolayers are of the order of 10^{-7} cm/s.

1.3.3 Apparent permeability coefficient (P_{app}) calculation

The apparent permeability coefficient (P_{app}, unit: cm/s) is determined from the amount of molecule transported per time, according to the following equation (Equation1):

Equation 1 $$P_{app} = \frac{\frac{dQ}{dt}}{AC_0}$$

Where dQ/dt is the rate at which the solute is transported across the barrier (mol/s), A is the surface area of the filter (cm^2) and C_0 is the initial concentration of the solute in the donor compartment (mol/cm^3). This equation relies on the following assumptions (49).

First, the system has to fulfill with sink conditions, implying that a molecule reaching the receiver chamber will not undergo back-diffusion into the donor. In practice, this condition is considered fulfilled if the concentration in the receiver compartment does not exceed 10% of the concentration in the donor compartment. Secondly, cellular retention and substantial losses of solute in the system are not taking into account (this assumption results from considering that the amount of solute that was transported across the barrier is equal to the amount measured in the receiver compartment) (24, 49).

In most cases, a single time point is performed in the experimental evaluation of P_{app}. The apparent permeability coefficient is than calculated from the accumulation of solute in the receiver compartment during that time interval, considering the concentration of solute in the donor compartment at t=0 as the driving force. In this approach it is not possible to evaluate whether the assumptions considered in the model are followed or not.

The methodology may be significantly improved if the accumulation of solute in the donor and receiver compartments is followed over time. Under those conditions it is possible to evaluate whether sink conditions are observed (when the amount transported is proportional to the time interval), and if the amount transported into the receiver compartment is equal to that leaving the donor compartment (in which case no significant retention/degradation by the cells or binding to the apparatus. In this case, equation 1 may be modified to equation 2, considering the concentration of solute in the donor compartment correspondent to that sampling time.

Equation 2 $$P_{app}(t) = \frac{\frac{Q(t+\Delta t)-Q(t)}{\Delta t}}{AC_D(t)}$$

In this approach, distinct values of P_{app} are calculated, one for each time point taken. The value considered for P_{app} may be calculated from the average of the distinct values obtained. It is however highly recommended to evaluate first any systematic time dependence. A time dependent increase in $P_{app}(t)$ is indicative of significant cell retention, while a time dependent decrease is strong evidence for non-sink conditions.
The concentration in the donor compartment at the beginning of sampling interval, may be obtained experimentally or calculated from that at t=0 and the cumulative amount of solute removed from the donor compartment (due to sampling and to transport into the acceptor compartment and/or sequestration by the cells and binding to the apparatus). Usually, the concentration in the donor compartment is not experimentally evaluated at intermediate times, being calculated assuming negligent sequestration by the cells and apparatus. At least at the end point it is very important to experimentally evaluate the amount of solute in both compartments and evaluate the conservation in the total amount of solute (% recovery). Recoveries much smaller than 100 % indicate significant sequestration by the cells and/or solute degradation, or binding to the apparatus.

The cumulative accumulation of solute in the receiver compartment (FA_{cum}) is calculated with equation 3, taking into account the time dependent concentration of solute in the donor compartment (the driving force for transport) and the amount of solute removed from the system due to sampling ($f=(1-V_S/V_R)$, where V_S is the sampling volume and V_R is the total volume of the compartment being sampled (25).

Equation 3 $$FA_{cum}(t_k) = \frac{1}{A}\sum_{k=1}^{i} \frac{Q(t_k) - fQ(t_{k-1})}{[C_D(t_{k-1}) - C_D(t_k)]/2}$$

The value of the observed permeability coefficient at a given time *t* is obtained from equation 4:

Equation 4 $$P_{app}(t) = \frac{FA_{cum}(t)}{t}$$

As discussed above with respect to equation 2, if $P_{app}(t)$ is not dependent on time, the average value should be considered, or alternatively, the slope of the best fit for a linear dependence of $P_{app}(t)$ on t. If systematic variations are observed, the validity of the assumptions should be evaluated and adequate actions should be taken to guarantee the adequacy of the model used.

One possible action that may be undertaken in an attempt to guarantee the validity of the assumptions (sink and no sequestration), is the addition of binding agents to the transport media. Because only the free (unbound) solute is available for permeation, the addition of binding agent to the receiver compartment reduces the transport in the backward direction and may be followed to guarantee sink conditions. On the other hand, the addition of binding agent to the donor compartment will decrease the amount of solute available to permeate and will therefore decrease P_{app}. To obtain the intrinsic permeability of the solute it is necessary to consider only the concentration of free solute as the driving force in equation 1.

In some cases, the addition of a binding agent may lead to an increase in the observed P_{app}.(50). This is an indication of extensive solute aggregation and/or binding to the apparatus when in the absence of the binding agent (51).

Possibly because of the added complexity and poor characterization of the system, the above corrections are only seldom applied, P_{app} being calculated from equation 1 directly (24).

Contribution of the filter to the measured P_{app}

In the permeability assay across a cell monolayer, the filter insert serves as a support for the monolayer. The filter can be a source of resistance for the transport of the solute and thus, the transport in the absence of cells in the membrane support should be characterized.

The observed resistance through the cell monolayer supported in the filter ($1/P_{app}$) may be decomposed in terms of several mass transfer resistances according to equation 3, where $1/P_f$ is the resistance imposed by the filter *plus* the resistance due to the presence of an unstirred water layer (UWL), and $1/P_c$ is the resistance imposed by the cell monolayer (52)

Equation 5
$$\frac{1}{P_{app}} = \frac{1}{P_f} + \frac{1}{P_c}$$

The contribution of the filter *plus* that of the UWL may be obtained by performing permeation experiments in the absence of a cell monolayer. The effective permeability coefficient through the cell monolayer may then be calculated.

The contribution of the UWL is incorporated in the above equation as it is present in both permeability experiments (with and without the cell monolayer). The thickness of

the UWL is strongly dependent on the stirring conditions, and this may affect significantly the value obtained for P_{app} (53, 54).

1.4 Rationalization of *in vitro* permeability data from Caco-2 assays

The Caco-2 model has been thoroughly used by the scientific community as a simple reference model in the prediction of drug permeability and absorption in humans. Determination of *in vitro* P_{app} in Caco-2 cell monolayers has become a routine aspect of many drug discovery programs. Nevertheless, even with the advances and improvements, experimental evaluation of P_{app} in Caco-2 assay could be laborious, time (longer culture period) and cost consuming as well as difficult to be performed in an high-throughput way. Therefore, before testing the compound in the system it would be of great value if the permeability through Caco-2 monolayer could be predicted from the structure of the compound.

The extensive use of this model has generated a large amount of data, which could in principle be used to obtain Quantitative Structure Property Relationships (QSPR). Those QSPRs could then be used to estimate permeability data, reducing significantly the time and costs required in drug discovery and development. The quantitative prediction of permeation from the structure of the drug candidate accelerates the selection of hits with better *in vivo* efficacy at early stages in drug development. Several studies have addressed the establishment of structure-permeability relationships based on experimental P_{app} values from Caco-2 assays published in the literature for a set of compounds (55). However, the correlations found when considering structurally unrelated compounds are poor and show little predictive value. This results mostly from data inconsistency and small size of the experimental dataset values used to derive them. Experimental P_{app} values in Caco-2 monolayers of the chosen compounds were usually pooled from data available in the literature. The discrepancy between the measure permeability coefficients reported by different laboratories for the same compounds is very large, often differing by several orders of magnitude. High interlaboratory variability in Caco-2 permeability results have been highlighted, although experimental protocols have already been supplied. This precludes the use of this information to obtain QSPR that may be reliably applied to predict drug's bioavailability.

In addition, interpretation of the results from permeability assays has been overly simplified. The rationalization of data from Caco-2 model is essential for a correct interpretation and requires a full understanding of both the strengths and limitations of the assay. Obtaining more consistent data will enable reliable comparisons between permeability values obtained from different researchers and protocols, and facilitate the development of *in silico* models truly predictive of intestinal absorption.

1.5 Interlaboratory Variability

1.5.1 Sources

Regarding the Caco-2 maintenance and transport experiments, much dissimilarity in culturing and experimental conditions used in different laboratories can be identified in the literature. Variations in culture and transport conditions can influence morphology and absorptive characteristics of Caco-2 monolayer and, ultimately, the outcome of the transport experiments (22, 56-61). Consequently, there are interlaboratory differences in the P_{app} measurements of permeability assays. Sources of this variability have been extensively reviewed (56, 57, 62) and some key points are summarized below.

Interlaboratory variability can be attributed to factors related with the cell line itself and with cell culture conditions (59). Due to the cellular heterogeneity of the Caco-2 cell line, when exposed to different selection pressures the cells differentiate into subpopulations with variations in cell morphology, biochemical, and transport properties (59, 60, 62, 63). Culturing conditions such as the degree of confluence, passage number, seeding density, filter support or culture medium are some of the factors that can select for different cell populations (56, 58-62, 64). Variable culture conditions and different numbers of passages between laboratories may result in an inconsistency in cell characteristics and properties, leading to high variability in its performance, poor experimental reproducibility and ambiguous results (61, 65).
Thus, it is important the standardization of culture procedures and use cells with similar passage number (defined number of passages) for related experiments to reduce intrinsic Caco-2 variability (59).

The variability in P_{app} values encountered can be also attributed to distinct experimental procedures during the transport assay (56). In fact, there is a plethora of factors related to the experimental setup that can influence the outcome of the assay. These factors include multi-well insert assay plates (12 or 24 Transwell), filter support materials (polycarbonate or polystyrene), sampling times and method (replacement or transfer), composition of the transport media, sink conditions, stirring rate and P_{app} calculation (49, 53, 56, 66). Also, the acceptance criteria in terms of monolayer integrity (measured as TEER value and/or P_{app} of mannitol or LY) differ between laboratories and is not always explicitly indicated (8).

Composition of transport media

In general, the majority of permeability studies use buffered saline solutions (e.g., Hanks' balanced salt solution (HBSS)) as transport media. Changes in the composition and properties of aqueous buffers have been proposed to improve the performance of *in vitro* Caco-2 model and overcome some shortcomings as well as ensure the use of more biologically relevant media (56, 66).

Selected pH

Commonly, the pH of the buffer is neutral (7.4) in both apical and basolateral chambers. However, the lack of pH gradient does not reflect the physiology of the gastrointestinal tract, and some studies employed different pH values for apical pH 6.0 (or 6.5) and basolateral pH 7.4 mediums (67). Work by Yamashita and colleagues, compared permeability values in the Caco-2 system of several dugs obtained in the presence and absence of a pH gradient (68). Their investigations revealed differences in the apparent permeability attributed to both differences in drug ionization/partitioning to the membrane and modification of carrier-mediated transport (68).

Solubility enhancers

An additional insurgent problem is the low solubility of the drug under study in the aqueous transport buffer. In such cases, apparent permeability coefficients can be misleading due to uncertainty regarding the exact concentration of drug in the donor

solution. For this reason, solubility-enhancing agents have been employed in Caco-2 experiments of poorly-soluble drugs, namely co-solvents (eg.DMSO, propylene glycol), bile acids and serum albumin (69). Although concerns exist regarding their cytotoxicity and tight junction disruption, the co-solvents have shown to be compatibility with Caco-2 monolayers up to a well-defined concentration which depends on the co-solvent (eg. 1% for DMSO) (68, 69). These additives are included in the apical and/or basolateral compartment. Addition of a bile acid component (eg. taurocholic acid) into the apical medium may have a beneficial effect in solubilizing these compounds as well improve even more the biorelevance of the Caco-2 model (68). The impact of solubilizing agents on drug permeability *via* mechanisms unrelated to drug solubilization is not fully understood.

Inclusion of BSA

Combined with limited solubility, the poorly water soluble and especially strongly lipophilic compounds have propensity for nonspecific adsorption to the plastic surfaces of the apparatus and accumulation within the cell monolayer, during the permeability assay (69, 70). Collectively, this results in significant drug loss and reduced recovery from the test system and/or the lack of quantifiable concentrations in the receiver sample to permit analysis. Specifically, the concentration gradient established (driving force) may be significantly smaller than that calculated from the total concentration in the donor compartment, and the concentration in the receiver compartment may be artificially reduced, both leading to an underestimation of the permeability coefficient. In the extreme, for very lipophilic solutes, the rate of permeation may become limited by the partitioning of the solute out of the cells (21, 68). Krishna et al reported retentions in Caco-2 cells of 54% for lipophilic compounds (71). Therefore, these issues and the low mass balance or recovery invalidates the determination of accurate and reliable P_{app} values (49)

The verification of sink conditions in a permeability assay is of major importance. In its absence, the apparent permeability coefficient obtained will depend strongly on the sampling intervals and method (16). For solutes with low aqueous solubility and/or high permeability, sink conditions cannot be taken for granted, even when the amount of solute in the receiver compartment is smaller than 10 % of the total solute introduced in the donor compartment. This difficulty in *in vitro* Caco-2 assays can be overcome through addition of serum albumin (BSA or HAS) to the receiver compartment The inclusion of serum albumin avoids the saturation of the acceptor compartment by

effectively decreasing the free concentration of the drug, which is crucial for the case of solutes with low aqueous solubility. Also, the decrease in the concentration of free solute decreases the back-flux of the compound to the donor compartment, which is crucial for the case of compounds with high permeability.
Addition of 4% BSA has been proposed to be most relevant for *in vivo* conditions (50).

1.5.2 Consequences on P_{app} values

The heterogeneity of Caco-2 cell line along with differences in the assay conditions, have led to a large variability in the values of P_{app} obtained for the same drug among laboratories (65) (61). Values of P_{app} for Propranolol, a compound highly permeable, can vary from 3.3 to 110. For Terbutaline, which have low permeability, the values for P_{app} can vary from 0.2 to 2 (65). Substantial differences were found across different laboratories for P_{app} values both for high and low permeability compounds.

What does this variability mean for investigators using Caco-2 permeability assays? Lee et al. demonstrate in what way the quantitative differences in Caco-2 permeability results from several laboratories can influence the prediction of intestinal absorption of drugs (65). These differences were assessed by determining the root mean square error (RMSE) values between the datasets. They determinate a RMSE as high as 0.581 between the P_{app} values experimentally obtained by them and other laboratory. Therefore, it is clear that Caco-2 permeability results should not be directly compared across different laboratories as it can mislead interpretation and the subsequent predictions (65).

1.5.3 Solutions for interlaboratory variability

Overall, standardization is crucial to reduce variability and improve the assays predictive ability for *in vivo* absorption (72). Also, it will prevent that each compound would be analyzed and evaluated by its own specific experimental set-up. Moreover, well-defined acceptance criteria (e.g., monolayer integrity, TEER) and transport studies with 10-20 reference compounds have been suggested for validation of the model and ensure method suitability (73) Ideally, a set of reference compounds should cover a

broad structural and physicochemical space and range of solubility/ permeability, with known *in vivo* human fraction absorbed. The objective is finding similar trends and rank-orders relationships between permeability values and human intestinal absorption for known reference compounds. Therefore, each experimental system must be calibrated with reference compounds before any permeability assessment with unknown compounds can be made.

Refinements and optimization of the *in vitro* experimental conditions, described in the previous section have been done to alleviate experimental obstacles and improve Caco-2 permeability assays. Nevertheless, this can give rise to experimental results of questionable validity if the data were not correctly interpreted. A thorough understanding of the rationale underlying these problems could certainly help putting the results in the proper perspective. Thus, it is essential to know the system and have accurate information regarding solute ionization, solubility, interaction with the cell membrane and serum albumin (both equilibrium and kinetics). On the basis of such an understanding, the interpretation of results of Caco-2 permeability study may be improved and made easier the comparison of experimental data obtained in different (but well defined) conditions.

Up to now, limited and qualitative data is available on the impact that these conditions may have on P_{app} values. For example, several studies determine the effect of adding BSA (51, 68, 74). P_{app} values were usually substantially decreased by the presence of the protein. If not quantitatively taken into account, this may result in erroneous permeability prediction once the intrinsic P_{app} of the compound is not changed. While in most cases it is not possible to quantitatively compare the data obtained following different approaches, an attempt to establish a reliable quantitative comparison needs to be developed.

The addition of BSA to the transport media is particularly useful in those permeability assays, to avoid aggregation of hydrophobic solutes, decrease binding to the apparatus, and to ensure sink conditions. Additionally, serum albumins are usually present in the *in vivo* system, in particular for the case of endothelia. The low cost and high purity of BSA available in the market (in particular it form free of fatty acids), makes it a better choice as compared with HAS. A quantitative evaluation of the effect of BSA in the system could therefore be a strategy to be employed to minimize the variability interlaboratories that partially limit the use of the Caco-2 model. One possible approach is to correct the observed P_{app} value using a correction factor obtained directly for permeability data generated in the presence of BSA. In this way, an intrinsic

permeability coefficient (for the free solute) would be obtained making possible the quantitative comparison of the permeability values obtained from different laboratories. This treatment would substantially decrease the uncertainty in the permeability of a given solute, opening the way to the use of the large amount of data available, to establish quantitative structure-permeability relationships and gain predictive value.

1.6 Aims of the study

The ultimate goal of this study is the establishment of QSPR, as a tool to understand and predict the rate of drug permeation through cell monolayers such as the BBB. To achieve this we have chosen to start with the Caco-2 model, because this is widely used and is usually assumed to correlate with permeability across cell monolayers in general. In addition, this is a stable cell line, relatively easy to work with, and well established protocols for the permeability assay have been disclosed (25). In contrast, *in vitro* models for the BBB using endothelial cells are recent, no well-defined protocols are available, and there is very little amount of permeability data available.

To achieve our goal, it is necessary to use a very large amount of data. Instead of trying the impossible task of characterizing a very large number of solutes, we have opted to characterize common alterations in the experimental protocol to be able to correct literature data obtained with distinct (but well defined) conditions.

Thus, in the first stage of this work the *in vitro* permeability assay using the Caco-2 cell model was implemented for the first time in our laboratory, following the most consensual protocol available in the literature (25). The morphology and the properties of the cell monolayer obtained were characterized using conventional tools, such as TEER, confocal microscopy and permeability of reference compounds. The transport through Caco-2 monolayers was also studied for the amphiphile NBD-C4 in both directions, A-B and B-A.

Secondly, the effect of the presence of serum albumin in the receiver only and in the receiver & donor compartment was quantitatively evaluated and rationalized in terms of the free fraction of NBD-C4. The P_{app} was interpreted taking into account the NBD-C4 interaction with components of the transport media as well as with the cell membranes, using data previously obtained by this group (75, 76), and a kinetic model recently developed by our group (21).

Lastly, permeability assays with NBD-C4 using endothelial cells obtained from Hematopoietic Stem Cells, have been undertaken. Comparison between the results

obtained with the two distinct cell models allows a better characterization of the properties of the different biological barriers, and an optimization of the drug's properties depending on their target tissue.

1.7 Why NBD-C4?

This amphiphile have a polar group, the fluorescent moiety 7- nitrobenz-2-oxa-1,3-diazol-4-yl (NBD) which is covalently bound to an alkyl chain with 4 carbons (NBD-C4) (**Figure 5**). The present work is focused on the transport study of this amphiphilic molecule through Caco-2 monolayers. The main reason for choosing this molecule was the large amount of high quality information regarding its properties and detailed kinetics and thermodynamics of interaction with lipid bilayers and serum albumin. For NBD-C4 it is known its solubility in water, the critical aggregation concentration, the partition coefficient towards membranes in distinct phases, as well as the association constant with BSA (**Table 1**) (76). Also, NBD-C4 fluorescence properties permit its quantification by HPLC with fluorescence detection for very small concentrations. In addition, the ionization behavior of NBD-C4 has been characterized, both in water and when associated with membranes, being in its neutral form at pH values close to 7 (pKa > 9) (76, 77).

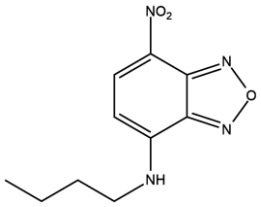

Figure 5 – Structure of NBD-C4.

Table 1 – Physicochemical properties, equilibrium parameters for the interaction with lipid bilayers and BSA.

CAC [a]	pka [b]		K_p [c]	K_B [d]	cLogP [e]
M	POPC	water	POPC	M^{-1}	
$2.5 \pm 0.3 \times 10^{-4}$	10.3	10	9.0×10^{2}	1.34×10^{4}	2.06

a) solubility of the monomeric form in aqueous solution, pH 7.4, at 25 °C

b) experimentally determined pKa values value obtained for NBD-C6

c) partition between an aqueous solution and POPC bilayers, pH 7.4, at 37 °C.

d) binding to BSA, pH 7.4, at 37 °C.

e) value calculated with MarvinSckech

Chapter 2

Material and Methods

2.1 Chemicals

Atenolol and LY were purchased from Sigma-Aldrich S.A. (Sintra, Portugal) (**Figure 6**). The fluorescent amphiphile NBD-C4 was synthesized in our lab as described by Cardoso et al (76). Bovine serum albumin was free from fatty acids from Applichem (Darmstadt, Germany). All organic solvents were of high purity grade (pro-analysis, HPLC or spectroscopic) from Sigma-Aldrich S.A. (Sintra, Portugal).

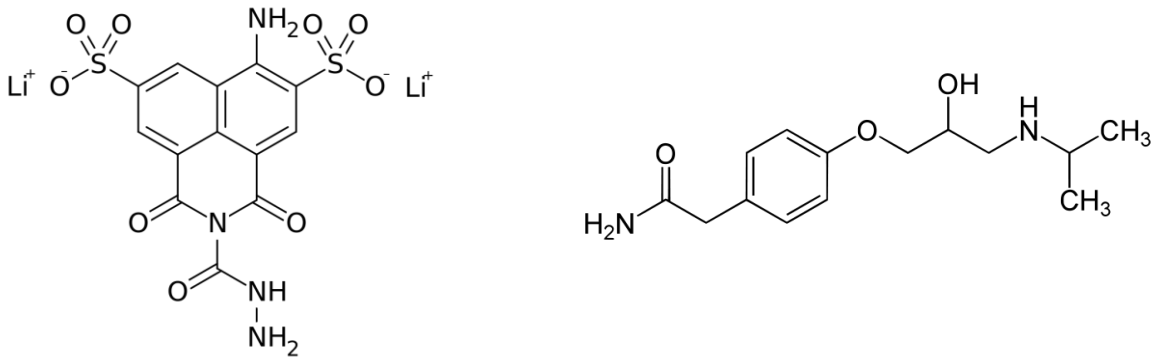

Figure 6 – Chemical structure of LY (right) and Atenolol (left).

2.2 Experimental Methods

2.2.1 Cell culture

Caco-2

The human colon adenocarcinoma cell line Caco-2 was a gift from Professor Paula Marques, purchased from the European Collection of Cell Cultures (ECACC, UK) at passage 44. Caco-2 cells of lower passage numbers (50–60) were used in this study. Cultures were tested for mycoplasma at the CNC facilities and found to be mycoplasma free. Cell stocks at passage 53 were prepared from the original vial and frozen by kepting one night at -80 ºC before being placed in liquid nitrogen. At time of the experiment, a vial was thaw and cells were grown for two passages before the seeding into Transwell inserts.

Cells were grown in 75 cm^2 culture flasks and maintained in Dulbecco's modified Eagle's medium high glucose (DMEM, Sigma- Aldrich) (4500 mg/L glucose with 2mM *L*-glutamine, without sodium bicarbonate), supplemented with 10% heat-inactivated fetal bovine serum (FBS, Gibco) and 1% non-essential amino acids (NEAA, Sigma-Aldrich), at 37 ºC in a humidified atmosphere of 5% CO2. Cells were subculture at 80-90% confluence twice a week (at a subculture ratio 1:4), using a 2.5% (wt/vol); trypsin-EDTA solution (10x solution, Sigma- Aldrich). The cells take 5min to detach from the culture flasks.

For transport experiments, the Caco-2 cell monolayer was cultured on Transwell polycarbonate filters inserts (0.4 mm pore size; 12 mm diameter, Costar) in 12-well plates as described previously (25). The cells used for seeding on the Transwell inserts were at 80-90 % confluence. After washing 2 times with PBS, the cells were suspended and centrifuged for 1100 rpm during 5 min. The supernatant was discarded and the cell pellet was resuspended with medium. The cell clusters were disaggregated into single cells by passing them 3 times through a syringe (23 gauges) before the cell counting. Cells were seeded on filters at a density $3x10^5$ cells/filter. The culture medium DMEM supplemented with 10% FBS, 1% NEAA and 1% penicillin (100units/mL) – streptomycin (10mg/mL) (Sigma- Aldrich) was replaced 6h after seeding and every second day thereafter. The monolayers were grown for 21 days prior to the permeability experiments.

Co-culture $CD34^+$-ECs/Bovine Brain Perycites

The *in vitro* BBB model was established according to published work (42). The $CD34^+$ cells were isolated from human umbilical cord blood and differentiated into endothelial cells (ECs) by cultivation in endothelial cell medium (EGM-2, Lonza) supplemented with 20% FBS (Life technologies) and $VEGF_{165}$ (50 ng/mL, PeproTech Inc) in 1% (w/v) gelatin-coated 24-well plates ($2x10^5$ cells/well). For each experiment, cells were expanded in 1% (w/v) gelatin-coated 100 mm Petri dishes (BD Falcon) in EGM-2 medium (with all supplements except FBS and gentamycin/amphotericin), supplemented with 2% FBS, gentamycin (50 mg/mL, Biochrom AG) and bFGF (1 ng/mL,Sigma-Aldrich).

The BBB model was established by co-culturing the $CD34^+$-derived ECs with bovine brain pericytes for 6 days. The bovine pericytes were initially grown on 60-mm gelatin-coated petri dishes and cultured in DMEM (Life Technologies) supplemented with 20% FBS, 2 mM Lglutamine, 50 mg/mL gentamycin and 1 ng/mL bFGF. The pericytes reached confluency after 2 day and were seeded at a cell density of $45x10^3$ in the

bottom of a 12 well plate (Costar) coated with 1% gelatin. One day after ECs were seeded at a density of $80x10^3$ onto the Matrigel-coated (diluted 1:48 in DMEM, BD Biosciences) Transwell inserts (0.4 mm porous size, 12mm diameter, Costar). Co-culture model was kept in EGM-2 medium supplemented with FBS (2%, v/v), gentamycin (50 mg/mL, Biochrom AG) and bFGF (1 ng/mL) for 6 days before permeability assays. The medium was renewed every 2 days.

The implementation of this model was performed at the Biomaterials and Stem Cell-Based Therapeutics laboratory of Dr. Lino Ferreira, with the supervision and support of Dr. Catarina Almeida.

2.2.2 Permeability assays

Transport experiments were performed as previously described (25) with slight modifications. The culture medium was changed 24h before the experiment. The Caco -2 monolayers were used for the experiments 21-29 days post-seeding, more specifically on days 22, 25 and 28. A filter insert without cells was included in each set of experiments. The transport medium used for the permeability studies was Hank's Balanced Salt Solution (HBSS, Sigma-Aldrich) buffer containing 10 mM HEPES and pH adjusted to 7.4. The HBSS was always pre-warmed to 37º C.

Prior to each experiment, cell culture media was removed from both sides of the filter inserts and the monolayers were washed twice with HBSS during 15 min under gentle shaking at 50 rpm with an orbital shaker (IKA-Schuettler MTS4) that was placed in an incubator at 37 ºC. The monolayer integrity of each filter was evaluated by measuring TEER using a Millicell -ERS system (Millipore) according to the manufacturer´s instructions. TEER values were measured in the HBSS at 37ºC before and after each experiment. The integrity control of the Caco-2 monolayers was also assessed with a paracellular marker LY (20µM). The permeability experiments with LY were done in separate monolayers and together with the compound to be tested.

Donor solutions with the compound of interest were prepared in HBSS and pre-warmed at 37 ºC. All the assays performed in this study were transfer experiments, where the receiver solution is exchanged at each sampling time. Thus, before the start of the permeability assays in the direction Apical to Basolateral (A-B), a 12 well plate is prepared, which contains HBSS (1.2 ml) for each filter in as many wells as there are sampling times. Initially, HBSS was decanted from monolayers and the compound solution was added to the donor compartment (0.45 mL). Immediately, an aliquot of

50 µL was withdrawn to an eppendorf and the filter insert is positioned into the first well and placed on an orbital plate shaker (50 rpm at 37 °C). Then, at each point in time the filter was moved from one HBSS-containing well to the next. At the end of the assay, 50 uL sample was taken from the donor compartment. For transport experiments in the Basolateral to Apical (B-A) direction, 1.2 ml of donor solution was placed on the basolateral side and HBSS (0.4 ml) in apical side. At each sampling time point, the solution on the apical side was decanted and replaced by new HBSS (0.4 ml). This approach is entitled “transfer” experiment.

When BSA was included in the assay, a BSA solution at 4 % (w/v) was prepared in HBSS. All the permeability assays without BSA, with BSA in the receiver and with BSA in the receiver and donor compartment were performed at day 22, 25 and 28, respectively.

Experiments were performed in triplicate. The samples were frozen within 1 hour and kept at -20 ºC until analyzed.

The endothelial permeability assays in the co-culture BBB model were performed in a similar way with slight differences. The transport medium used was EBM-2. The confluent monolayers of $CD34^{+}$-ECs, were used after 6 days in co-culture. TEER was measured in EGM-2. The experiments were performed under gentle shaking at 35 rpm with an orbital shaker that was placed in an incubator at 37 ºC and 5% of CO_2.

2.2.3 Preparation of compounds solutions

Individual stock solutions of compounds were independently prepared in methanol for NBD-C4 (200 µM), in miliQ-water for LY (6 mM) and in DMSO for AT (2 mM). To prepare the NBD-C4 solution (10 µM), the respective volume in methanol was collected from the stock solution and placed in a glass tube. Methanol was evaporated under a gentle stream of nitrogen and heat, producing a film. Then, the film was dissolved in the transport media to obtain the desire concentration. For LY solution (20 µM), the aliquot from the stock was directly added to the transport media. The working atenolol solution (100 µM) was prepared by diluting the stock solution in transport media at a final DMSO concentration of 0.5 %. The actual concentration of solute in the solutions was determined by UV-vis spectrophotometry using a molar extinction coefficient of 2.1×10^{4} $M^{-1}cm^{-1}$for NBD-C4, 1.2×10^{3} $M^{-1}cm^{-1}$for LY and 1.5×10^{2} $M^{-1}cm^{-1}$ for AT at 485 nm, 430nm and 279 nm, respectively.

2.2.4 Cytotoxicity assays

The viability of Caco-2 and ECs cells in the presence of all compounds and solvents used was evaluated prior to the permeability experiments. Cytotoxicity assays were performed with the same cell passage number as in transport studies (p. 50-60 for Caco-2). Cells were seeded in 24-well plates at a density of $5x10^4$ cells/well (both Caco-2 and ECs) and grown for 4 days in culture medium. Prior to the experiment, culture medium was removed and cells were incubated for 2h either with transport medium alone or including the compound of interest at the concentrations used in permeability assays. The assay occurred under orbital shaking in an incubator at 37 ºC. The respective culture medium DMEM/EGM-2 was used as negative control assay. Then, solutions in each well were aspirated, and the cells were incubated again for 4h with a resazurin solution (Sigma-Aldrich) in a cell culture incubator. The resazurin stock solution (0.1mg/mL in PBS) was diluted 10x in DMEM/EGM-2 and added to cells, 500 µL/well. The fluorescence signal from the reduced specie of resazurin (resorufin) was measured in a plate reader using 570/585 nm for excitation/emission.

Cell viability was calculated based on the measured fluorescence of the cells exposed to the negative controls, which represented 100% cell viability. Cell viability is expressed as a percentage of the control group. The experiment was performed once (in triplicate wells).

2.3 Analytical Methods

2.3.1 Fluorescence spectroscopy

The concentration of LY in the permeability assay samples was determined using a fluorescence microplate reader (Synergy, Biotek). After the transport assay, the LY samples from the receiver and donor compartments were placed in a 96-well plate for measuring. The volume used was 200 µL/well in two replicate wells for each sample. The samples from the donor compartment (50 µL) were diluted 10x with HBSS before adding to the wells. The fluorescence was read at 430/530 nm for excitation and emission wavelengths, respectively.

2.3.2 High Performance Liquid Chromatography (HPLC)

The concentration of the compounds Atenolol and NBD-C4 in the samples from the permeability assay was determined using a High Performance Liquid Chromatography (HPLC) system with a Diode Array (model G1315D from Agilent, USA) and Fluorescence detector (model G1321A from Agilent, USA). The injection loop was 200 µL and 300 µL of sample was injected to ensure complete replacement of the solution in the loop. The chromatographic separation of all compounds was performed in a reversed-phase C18 column (250 nm x 4.6 nm, Agilent) with a particle size of 0.5 µm and with a C18 pre-column (Agilent).

Specific HPLC conditions and eluents used are listed in **Table 2.** All compounds were separated in less than 10 min allowing for fast analysis. Donor samples were previously diluted 5x with HBSS to the volume of injection. For the samples containing LY as internal standard as well as the compound of interest, the mixture of the compounds was analyzed with the same mobile phase as indicated in Table 2 for the compound of interest. In all cases the retention time of LY is near 3 minutes. The two compounds were quantified by fluorescence, selecting a pair of excitation/emission wavelengths adequate for LY (430/530) until 6 minutes and the pair of wavelengths characteristic of the fluorescence of the compound of interest at longer times. Typical fluorescence chromatograms obtained are shown in **Figure 7**.

Table 2 - HPLC procedures for studied compounds.

Compounds	**Run time (min)**	**Mobile Phase (%)**		**Flow rate (ml/min)**	**Retenton time (min)**	**Fluorecence detection (nm)**		**UV detection (nm)**
		MeOH	miliQ-water			Ex	Em	
NBD-C4	0	50	50	1	8	450	520	467
	5	80	20					
	6	80	20					
	7	50	50					
	10	50	50					
Atenolol	10	MeOH 15	Buffer [a] 85	1	7	230	302	

[a] 50mM ammonium acetate with pH adjusted to 3 with acetic acid glacial.

The samples containing BSA were pre-treated to remove BSA before being injected into the HPLC system. To 100 µL of sample, 600 µL of ice-cold methanol (MeOH) was added to precipitate the protein. The samples were vortex for 5s and centrifuged at

12,000 rpm for 10min. The supernatant (400 µL) was taken to a new eppendorf and analyzed by HPLC.

The efficiency of this method was evaluated with regard to protein precipitation by following UV absorption of the supernatant. The method was also tested for the % recovery of the interest compound using NBD-C4. This was achieved through the comparison of the concentration of NBD-C4 in the supernatant of samples originally containing BSA, with that from samples with the same concentration of NBD-C4 dissolved in HBSS, both subjected to the same procedure. The recovery efficiency was at least 94 ± 9 %.

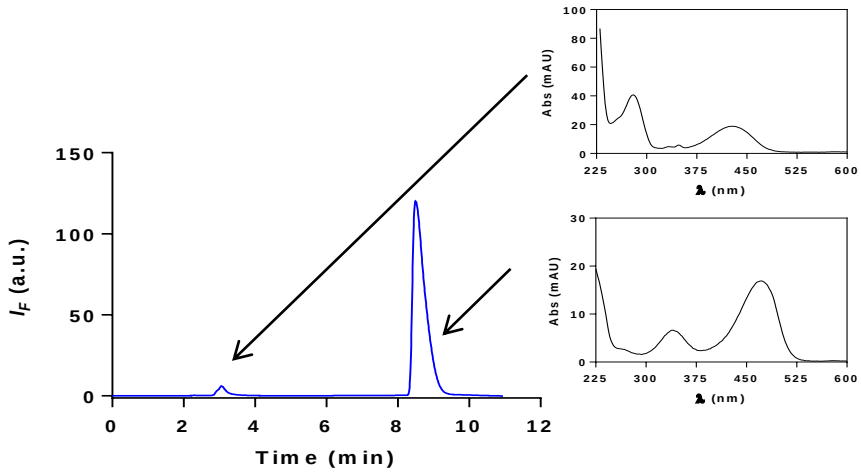

Figure 7 – Chromatogram obtained for NBD-C4 and LY. The first peak corresponds to LY (RT ≈ 3 min) and the main peak to NBD-C4 (RT ≈ 8 min). The absorption spectrum of the peaks is also shown.

2.3.3 Calibration curves

For the quantification of the samples, calibrations curves were constructed from the best linear regression of the chromatographic peak area versus concentration of compound (**Figure 8**). Several solutions covering the relevant experimental range of concentrations for each compound were prepared in HBSS. Linearity parameters of each calibration curve are described in **Table 3**.

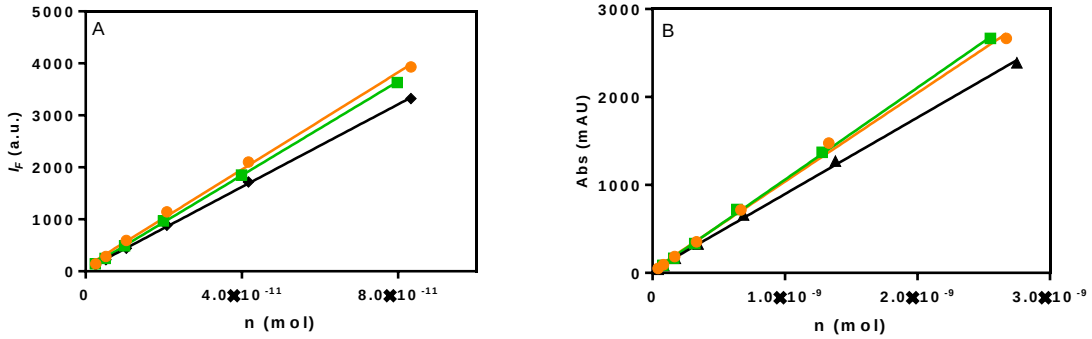

Figure 8 – Calibration curves obtained for NBD-C4. NBD-C4 was measured by A) fluorescence and B) UV-Vis. The graphs are the results obtained for three calibration curves.

2.3.4 Confocal Laser Scanning Microscopy (CLSM)

The morphology and integrity of cells monolayers was analyzed with confocal microscopy. The ZO-1 was detected using the ZO-1 polyclonal antibody with the secondary antibody *Cy3* Goat Anti-Rabbit IgG, purchased from Alfagene

For immunostaining, the cells were labelled and prepared at room temperature following a standard protocol. Briefly, the cell monolayers on inserts were washed twice with PBS (pH 7.4) and fixed in 4% paraformaldehyde (in PBS) for 10 min. After washing three times with PBS they were permeabilized with Triton X-100 (0.1%, w/v) for 15 min and washed again three times. Preparations were incubated with BSA for 30min and after, 1 h with the primary antibody (dilution 1:200) and with secondary antibody (dilution 1:100) for 30min in the dark. Cell nuclei were labeled with Hoechst 33342 stain (dilution 1:100). The filters was washed three times with PBS, cut and mounted on a glass slide with fluorescence mounting medium (Dako).

Confocal images were obtained on a Zeiss LSM 410 inverted microscope.

Table 3 - Linearity parameters for all studied compounds.

Compounds	Range (µM)		Slope (x 10^{-12} mol)		Intercept		Correlation Coefficient		LD (µM)		LQ (µM)	
	FLU	UV	FLU	UV	FLU	UV	FLU	UV	FLU	UV	FLU	UV
NBD-C4	0.01 - 0.5	0.5 - 10	43.9 ± 3.7	1.02 ± 0.09	54.7 ± 3.1	24.7 ± 7.85	0.9996	0.9993	0.02	0.4	0.06	1.2
LY	0.0002 - 0.02		61.5		1.85		0.9998		0.0005		0.0015	
Atenolol	0.025 - 5		4.36		10.36		0.9998		0.02		0.06	
	0.05 - 50		19.6		40.01		0.9991		0.03		0.1	

Chapter 3

Results and Discussion

3.1 Implementation of the *in vitro* Caco-2 cell model

After growing for 21 days on the filter supports, the Caco-2 cells are expected to be as a confluent and polarized cell monolayer with well-defined tight junctions (25). Nevertheless, it is important to first confirm the formation of a monolayer (and not multilayers), and to validate the barrier integrity (functional tightness) before proceeding with compounds testing.

Characterization and quality control of the Caco-2 monolayers growing on filter supports, complemented by confocal microscopy studies are essential to ensure reliable permeability measurements. Thus, a routine examination of each batch of cell monolayers should be performed prior the transport assays.

3.1.1 Characterization and evaluation of the Caco-2 cell monolayer

3.1.1.1 Caco-2 cell monolayer integrity

The properties of the Caco-2 cell monolayer as a barrier is commonly assessed in two steps: measuring the permeability to small ions (through TEER measurements) and the permeability of very polar molecules which are markers for paracellular permeability (such as the fluorescent molecule LY).

Caco-2 cells were grown for 21 days on filter inserts and on day 22 the TEER value of each insert was routinely measured. To confirm the presence of a cell monolayer, this parameter was compared to TEER of the filter support (in the absence of cells) (**Figure 9**). Caco-2 monolayers growing in our laboratory have TEER values of 411 ± 40 $\Omega.cm^2$ (n=30) at 37 ºC. The average value of the resistance across polycarbonate filters was 223 $\Omega.cm^2$ ranging from 217 to 229 $\Omega.cm^2$ (n=20). This value was subtracted to the total resistance across cells and we obtained standard TEER values of 188 ± 34 $\Omega.cm^2$ (n = 30) for the resistance of the monolayer.

The values obtained are not easily compared with those in literature because it is not always clear whether the reported value corresponds to the filter *plus* cell monolayer or to the monolayer itself. When comparing with the properties reported by Hubatsch et al, (265 ± 60 $\Omega.cm^2$) (25) we observed that the cell monolayer obtained by us is not as

tight. However, most of the preparations have TEER values above the *cut off* defined in the protocol followed by us (3) as being indicative of the formation of a confluent cell monolayer (TEER > 165 Ω.cm^2).

TEER values were also compared when a different batch of cells (post-defrosting) was used. **Figure 9** shows TEER results obtained for one assay plate (n=12) and for two additional assays plates performed on different days (n=30). The TEER value and the standard deviation associated was not significantly affected by the inclusion of multiple assays. The Caco-2 model shows good reproducibility for TEER measurement in our laboratory.

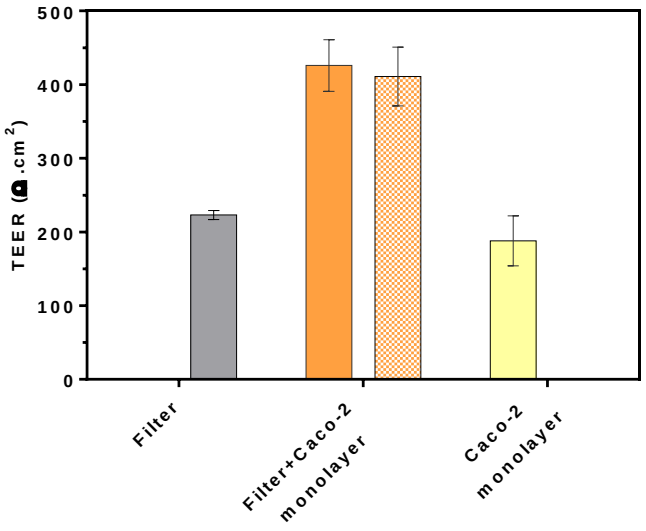

Figure 9 – TEER measurement of the Caco-2 monolayer: TEER of the filter support (grey, n = 20), Caco-2 monolayers in the filter support (orange, n = 12 or n = 30) and Caco-2 monolayer (yellow, n = 30) measured at day 22 in culture.

According to the protocol being followed, the Caco-2 model can be used for transport experiments for days 21 to 29 after seeding in the filter inserts. It is however not indicated whether the same filter may be used for several assays, and if so, what is the procedure that should be followed between assays. We have performed some preliminary studies that show that the cell monolayer reestablish the barrier properties if maintained in culture media for two days after the permeability assay (data not shown). Taking this into account, we chose to perform the permeability assays three times on the same monolayer insert, specifically on days 22, 25 and 28. Thus, it was necessary to check the suitability of each monolayer at the respective experiment day

before testing the compounds. The TEER measurement obtained at the different days is shown in **Figure 10**.

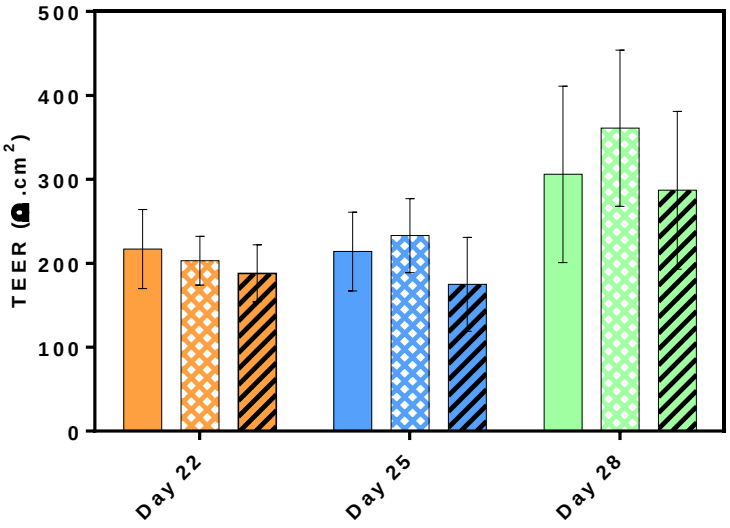

Figure 10 – Barrier function of Caco-2 monolayer at the different experiment days. TEER measurement of the Caco-2 monolayers at day 22 (orange), 25 (blue) and 28 (green). Solid-pattern n = 3 (control, HBSS only), chess-pattern n = 12 (one assay plate) and scratched-pattern n = 30 (three assay plates).

It is observed a systematic increase in the TEER values with the time of differentiation of the monolayer on the filter supports. The resistance increased from 188 ± 34 $\Omega.cm^2$ at day 22 to 287 ± 94 $\Omega.cm^2$ at day 28 (n=30). We can also see a significant increase in the standard deviation associated with this parameter, from 22 % to 34 % for a single day set of experiments (n=3) and 18 % to 33 % when including two additional sets of experiments (n=30). This indicates that the Caco-2 cell monolayer has a larger variability on day 28 and/or that the treatment applied to the cell monolayer during this period is affecting in a non-systematic way their properties. The results shown on **Figure 10** correspond to a single plate treated only with HBSS for 1 h (control) (n=3), 3 filters in a single plate treated with HBSS and 9 filters with test compounds (n=12), and plates prepared from new cell preparations including also the controls and filters where the permeability of test compounds was evaluated (n=30). The control monolayers exhibited the same trend in the variation of TEER values between days. This indicates that it is the time after cell seeding in the filter that is affecting the behavior of the cell monolayer, not an effect of the tested compounds. A sistematic increase in the TEER value with time even after day 21 has been reported before, in the original papers that explored this assay (23).

The barrier integrity of the Caco-2 cell monolayer was also assessed by evaluating its permeability to the paracellular marker LY. The transport of LY was performed at days 22, 25, 28 in the same monolayer inserts where TEER was measured (**Figure 11**)**.**

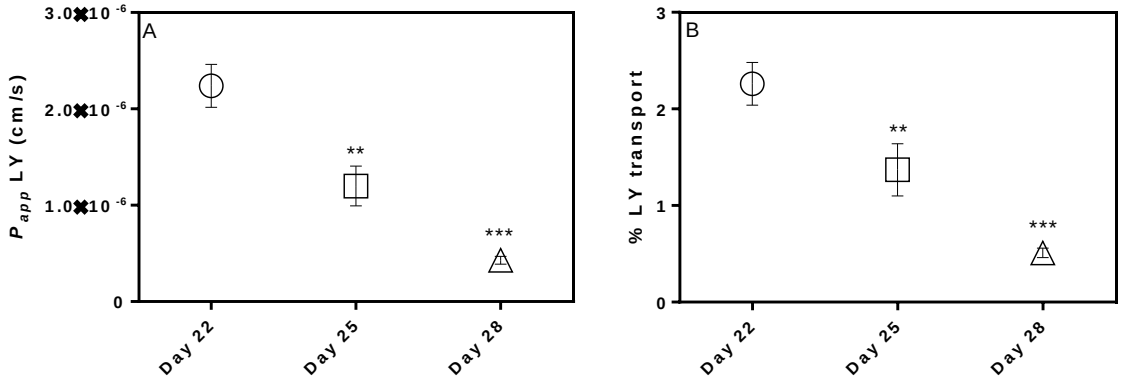

Figure 11 –Caco-2 monolayer integrity at the different experiment days. A) Permeability of the paracellular marker LY across the monolayer after 60 min. B) Percentage of LY transported after 60 min. The results are the mean ± SD of three monolayers. Asterisks indicate significant difference from the day 22 ($p < 0.01$).

LY permeability experiments were conducted over 1 hour and the P_{app} value was calculated as described in section 1.3.3. Small values of LY P_{app} offer evidence for monolayer tightness. It is usually considered that less than 0.5 % of the LY added to the donor compartment may be transported across the cell monolayer per hour. In our laboratory, the P_{app} of LY at day 22 was 2.2 ± 0.2 x 10^{-6} cm/s (n=3) which corresponds to 2.26 ± 0.22 % of LY transported across the Caco-2 monolayer per hour. This value was unexpectedly high given the TEER values obtained. The value obtained for the apparent permeability coefficient is significantly higher than previously reported in the literature (0.05 ± 0.01 x 10^{-6} cm/s (74)). When the time of differentiation is increased, at day 28, the P_{app} of LY across the monolayer was significantly smaller (P_{app} = 0.43 ± 0.04 x 10^{-6} cm/s, n=3), corresponding to 0.51 ± 0.05 % per hour. Both TEER and LY permeability indicate an improvement on the tightness of the cell monolayer from day 22 to 28.

In the present study, the increase on TEER measurements was consistent with a decrease in the permeability of LY, at the different days tested. The correlation between the two parameters is quantitatively evaluated in **Figure 12A**. An inverse relationship was observed between the TEER and P_{app} of LY under the experimental

conditions used for the assay, higher LY permeability values corresponding to lower TEER values. When the resistance to LY transport ($1/P_{app}$) was plotted against the TEER values, the correlation is even more evident (**Figure 12B**).

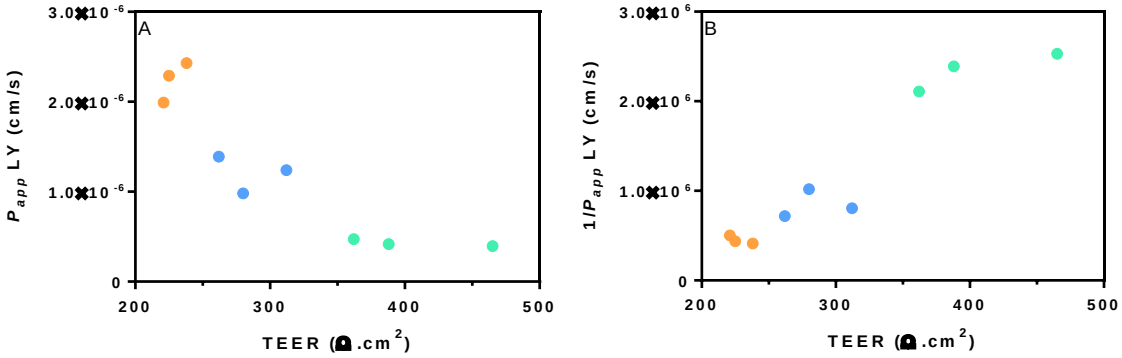

Figure 12 – Correlation between the permeability of LY and TEER. The P_{app} value of LY (A) and the inverse of the P_{app} of LY (resistance) (B) plotted against the TEER measurements of Caco-2 monolayers at day 22 (orange), 25 (blue) and 28 (green). Each point represents one insert.

It should be noted however that the information obtained by the two parameters is not redundant in what concerns evaluation of the cell monolayer properties. Namely, all cell monolayers on day 25 were considered tight in terms of TERR (> 165 $\Omega.cm^2$), but not in terms of LY permeability (< 0.05 x 10^{-6} cm/s).

Therefore, the optimal evaluation of the Caco-2 monolayer integrity should include both parameters. Nevertheless, which gives the more reliable information regarding the quality of the monolayer? The parameters give different information. TEER reveals the resistance of ion passage through the paracellular pathway, while the permeability of the LY indicates the paracellular water flow and the pore size of the tight junctions (47). TEER measurements are non-invasive, simple and rapid. Even though, factors such as type of insert, temperature and measuring equipment can affect this measure, being more variable for routine use. The LY permeability is usually performed in 1 hour, which means that the tested monolayer are unusable for further experiments and have to be discarded. To reduce the number and duration of incubations, the assay with LY may be performed in simultaneous with the compound to be studied. Possible effects of one compound on the permeability of the other should be evaluated.

In this work we have also assessed the barrier properties of the cell monolayer by measuring the permeability of atenolol, one of the common reference compounds used

to validate the Caco-2 model. Atenolol is a weak base that is passively transported and has low permeability across the Caco-2 monolayer (67).

The transport of atenolol was performed at day 22 and samples of the basolateral compartment were taken after 10, 30, and 60 min The experiment was performed under sink conditions which allow the P_{app} to be calculated as in section 1.3.3.

In our laboratory, we obtain a permeability coefficient for atenolol of 4.7 x 10^{-6} cm/s, (n=3) which is high when compared to reference data in the literature (**Table 4**). This result is in agreement with the relatively high permeability of LY obtained at day 22.

Table 4 – Permeability assay and the respective parameters of atenolol across the Caco-2 monolayer.

TEER	**Recovery**	**Transport rate**	P_{app}	
$\Omega.cm^2$	%	%	(x 10^{-6}) cm/s	
			our laboratory	from literature (27, 67)
170 ± 5	93 ± 11	5.0 ± 0.7	4.7 ± 0.7	0.3 - 1

The results are the mean ± SD of three experiments.

3.1.1.2 Confocal microscopy

Although TEER and LY permeability measurements gives important evidences on the presence of well-defined tight junctions and characteristics of the cell monolayer, morphological studies helps to validate these features. Confocal microscopy images of Caco-2 cell monolayers should reveal a single cell layer, without multilayer formation, with confluent cells and an extensive network of tight junctions between them. Unfortunately, the majority of the reports in the literature using the Caco-2 model do not show the confocal microscopy images resulting from the morphological study.

Cytoskeleton, cell nuclei and tight junctions of 21-days differentiated monolayers were investigated by confocal microscopy (**Figure 13**). Images showed that Caco-2 cells were in a monolayer on the filter support, but not at full confluence. Also, the cell monolayer was not uniform, exhibiting some holes. The localization of the ZO-1 protein at the tight-junctions of Caco-2 cells shows a discontinuous expression of ZO-1 between the cell-cell contacts. In the same way, the ZO-1 staining is not vertically aligned with the cell nucleus. All together this indicates that the cells are not fully matured and differentiated at day 22. The cell density is not that required for full maturation and therefore, cells continue to divide.

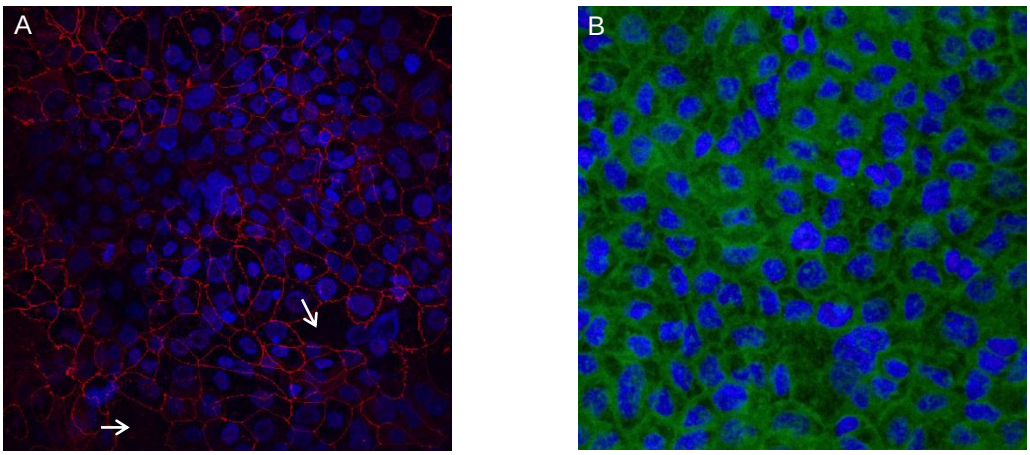

Figure 13 - Typical confocal micrograph (from 3 filters analyzed) showing the morphology of the Caco-2 monolayer after 21 days in culture. Images were obtained at 20x objective. A) Immunocytochemical staining of the tight junction protein ZO-1 (red) and nucleus were stained with Hoestch (blue). The blank arrows show a hole into the monolayer. B) Phalloidin staining for actin filaments is represented in green.

At day 21, the Caco-2 cell monolayers prepared by us following the protocol reported in literature (25) show incomplete differentiation, are not full confluent and do not show well-developed tight junctions. These results from confocal study are in agreement with the high permeability of the paracellular marker LY and low TEER values (although passing the quality control threshold). This may also explain the improvement in the cell monolayer properties from day 21 to day 28, although a morphological evaluation at days 25 and 28 must be performed before any conclusion may be taken.

3.1.2 Effect of the experimental conditions on Caco-2 monolayer viability and integrity

The viability of the Caco-2 cell monolayers during the permeability experiments is a prerequisite for reliable permeability measurements, as high permeability values can result from cell death and subsequent loss of monolayer function. The compound concentration and the co-solvent that are used might affect the viability and integrity of the cell monolayers. Also, stirring the inserts at a too vigorous rate may compromise the integrity of the cell monolayer.

The cytotoxicity test was performed incubating the Caco-2 monolayer with the compounds to be tested for 2 h at 37°C, in the presence and absence of stirring (**Figure 14**).

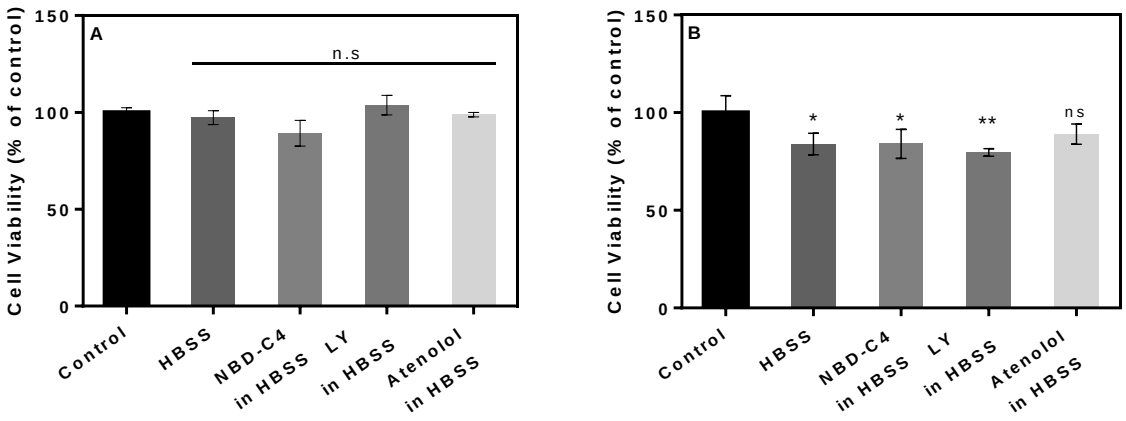

Figure 14 – Effect of the experimental conditions in Caco-2 viability: Cell viability was assessed after 2h of incubation with the compound in A) the absence of stirring and B).with a stirring rate of 50 rpm. Results are mean ± SD of three replicates. Significant difference from the control ($p < 0.01$).

The studied compounds induced no toxic effect on the Caco-2 cells at the used concentrations. No decrease on the cell viability was observed with DMSO at a final concentration of 0.2 % used in atenolol solution.

When a stirring rate of 50 rpm was applied, the cell viability decreased. The agitation could be a problem in the permeability assay. There is a large amount of information in the literature regarding the effect of stirring on the permeability observed, increase in P_{aap} with speed of stirring (53) It is usually considered that the increase in permeability is due to a concomitant decrease in the unstirred water layer (UWL) adjacent to the cell monolayer.(54) Unfortunately, to our knowledge a systematic evaluation of the effects of stirring on cell viability and morphology as not been done. It should be highlighted that the speed rate used by us (50 rpm with an orbit of 3 mm) is the minimum value reported in the literature and as low as can be done with the equipment commercially available.

The effect of the experimental conditions used on the permeability assays on monolayer integrity was evaluated by measuring the TEER before and after each experiment. The value measured at the end of the experiment was statistically different from the value of TEER before the experiment (**Figure 15**).

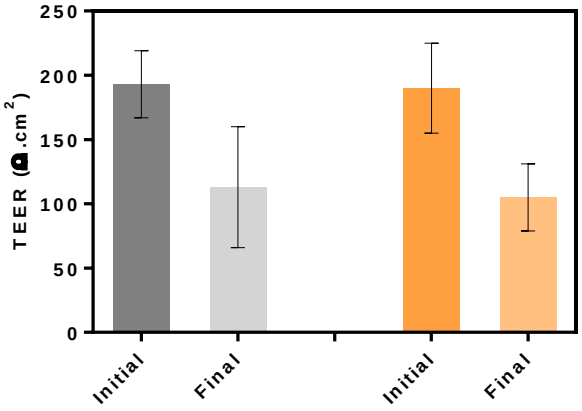

Figure 15 – Effect of the experimental conditions on Caco-2 monolayer integrity. Evaluation of TEER before and after the permeability experiment at day 22. Control filters (HBSS only) are presented in grey (n = 3) and the bars in orange are the results obtained on permeability assays (n =30).

The initial and final TEER values were of 188 ± 35 and 101 ± 26 Ω.cm2 (n = 30), respectively. There is a decrease of approximately 45 % in the TEER values. The same drop in the resistance was observed in the assay controls. This indicates that de sampling method and times do not affect the TEER. Indeed, the agitation seems to be the experimental condition that was affecting the TEER.

However, the TEER value exhibits a recovery at day 25 and also from the day 25 to 28 (**Figure 16**).

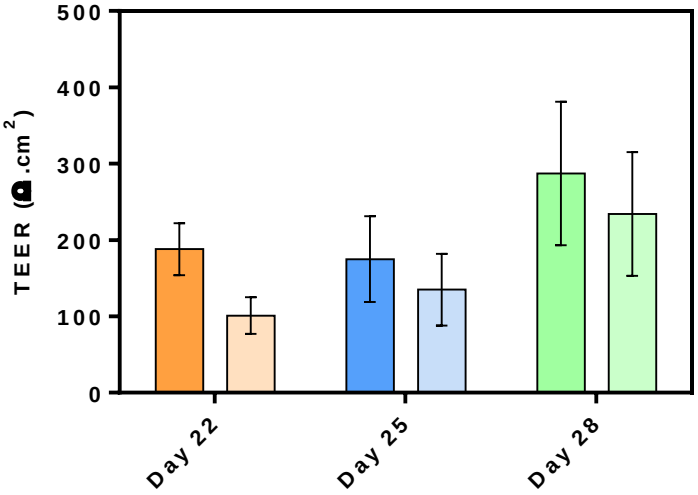

Figure 16 – Recovery of TEER value with the differentiation day. Evaluation of TEER before (dark colors) and after (light colors) the permeability experiment at day 22, 25 and 28. The measures are the results obtained on permeability assays (n =30).

3.2. Transport of NBD-C4 across *in vitro* Caco-2 cell monolayers

After characterization of the Caco-2 model, we have proceed to the study of the transport of NBD-C4 across the cell monolayer. As it is the first time that permeability assays in the Caco-2 system were carried out for this amphiphile, the conditions of the transport experiments had first to be designed. For this, we had in consideration the NBD-C4 properties (**Table 1**) and the predictions of the rate of passive permeation of this amphiphile across a cell monolayer by the kinetic model developed by us.

At the concentration used, (10 µM) NBD-C4 is soluble in HBSS in the monomeric form.

In order to choose the optimal time interval between each sampling, we need to have some knowledge about the transport rate of the NBD-C4 across the cell monolayers. According to the simulations in our kinetic model, NBD-C4 is expected to exhibit a permeability coefficient in the order of 10^{-4} cm s^{-1}, leading to 10 % transfer from the donor to the acceptor compartment in approximately 5 min (21). The NBD-C4 was therefore expected to be rapidly transported across the cell monolayers. Sampling has to be taken at short time intervals to ensure that sink conditions are maintained, that is, negligible concentration of NBD-C4 in the receiver side at the sampling times. Taking this into account, the sampling was performed at time intervals of 2.5 min for a total of 10min. This was considered the smallest sampling interval that still allows for maintenance of the experiment conditions, namely the temperature at the permeability assay apparatus. The sampling was obtained through transfer of the insert to new transport media in the acceptor compartment, in an attempt to further guarantee that sink conditions apply.

In some experiments we have added bovine serum albumin (BSA) to the transport media. A BSA concentration of 4 % (w/v) was used, which corresponds to the normal concentration of albumin in the serum and is that commonly used in *in vitro* Caco-2 permeability assays.

The transport of NBD-C4 was performed in both directions, apical to basolateral (A-B) and basolateral to apical (B-A), and in three different conditions. Firstly the transport was study in the absence of BSA. Next, we included BSA in the receiver compartment, which is the approach commonly used in the literature to mimic transport in the absorptive direction (intestinal lumen to blood, A-B). Finally, we have included BSA in both the donor and receiver compartment. The apparent permeability coefficient P_{app}

was calculated as done before for the standards (Equation 2, section 1.3.3) and interpreted taking into account the specific conditions of each experiment.

3.2.1 Transport of NBD-C4 in the A-B direction

Typical results obtained for the transport of NBD-C4 in the A-B direction without BSA are shown in **Figure 17**. The results are given as the cumulative amount of NBD-C4 transported into the receiver compartment versus time. The amount of NBD-C4 transported across the Caco-2 cell monolayers is proportional to the time interval. In the first 2.5 min of the assay, 3.6 ± 0.2 % of the initial amount of NBD-C4 in the donor was transported across the cell monolayer. After 10 min, 14-16 % of the amount of NBD-C4 added to the donor was accumulated in the receiver side. The conservation in the total amount of NBD-C4 was 95.4 ± 0.7 % at the end point of the assay. This recovery indicates that there was no significant cellular retention or adsorption of NBD-C4 to the Transwell system.

The cumulative amount was used in Eq. 2 to calculate the P_{app}. In the absence of BSA, the P_{app} for NBD-C4 was 8.8 ± 0.4 x 10^{-5} cm s^{-1} (n = 5).

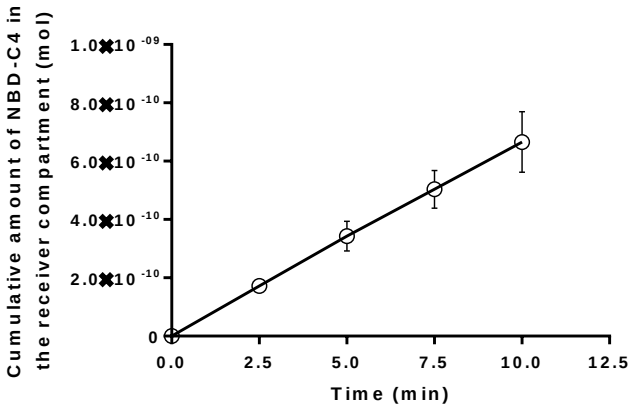

Figure 17 – Cumulative amount of NBD-C4 transported in the A-B direction without BSA. The accumulation in the receiver compartment was followed at four time points. The results are the mean ± SD of n = 5 experiments.

To evaluate the validity of sink conditions one should consider the ratio of the concentration of solute (available for transfer) in both compartments, and not the ratio in the amount of solute. As indicated above, during the first 2.5 min, on average 3.6 mol % of the NBD-C4 initially in the donor compartment was transported to the

acceptor compartment. Because the volume of the acceptor compartment is larger than that of the donor, this amount of NBD-C4 transported leads to a concentration in the acceptor compartment of only 1.2 ± 0.1 % of the initial concentration in the donor side. The limit for sink condition was therefore not exceeded. It should be noted that in those experiments each time interval is independent from the previous in what concerns sink conditions because sampling is made by transfer of the insert into a new acceptor solution.

To evaluate the effect of decreasing the fraction of NBD-C4 in the acceptor compartment available for transfer (thus reinforcing sink conditions) we have added BSA to the receiver compartment and measured the apparent permeability of NBD-C4 under this conditions. This is also relevant to evaluate the effect of this condition on the apparent permeability coefficient, as this is a common procedure on permeability assays.

3.2 2 Effect of BSA in the receiver compartment

The effect of adding 4 % BSA in the receiver compartment on the cumulative amount of NBD-C4 transported across Caco-2 monolayers are shown in **Figure 18**. The amount of NBD-C4 transported was 7.0 ± 0.1 % of the initial amount in the first time point. Thus, the presence of BSA in the basolateral side increases the accumulation of NBD-C4 in the acceptor compartment. This is expected to occur due to binding of NBD-C4 to BSA, which reduces the amount of solute available to transfer back into the donor compartment. Consequently, it is expected that the observed P_{app} increases slightly as compared to the P_{app} in the absence of BSA.

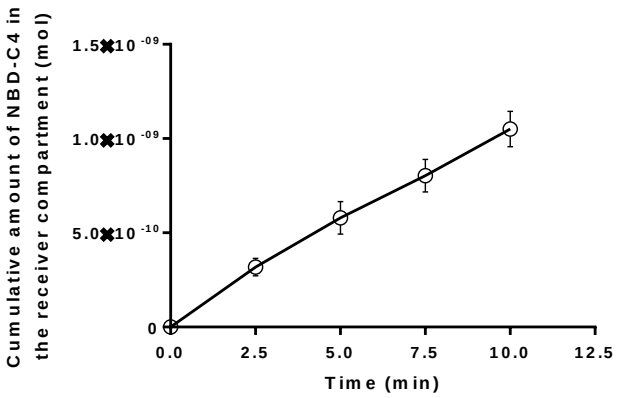

Figure 18 – Cumulative amount of NBD-C4 transported in the A-B direction with BSA in the receiver compartment. The results are the mean ± SD of three experiments.

When 4 % BSA was applied in the receiver side, the P_{app} calculated was $1.5 \pm 0.1 \times 10^{-4}$ cm s^{-1}. A significant increase on the P_{app} value of NBD-C4 was observed, by almost a factor of two. This increase caused by the inclusion of BSA was higher than expected, given the good sink conditions observed in the absence of BSA (see previous section). This observations may suggests the existence of experimental artifacts in the measured P_{app}. This will be further discussed below.

In this experimental condition, the NBD-C4 recovery was 100 ± 3 % compared to that obtained in the previous assay. The addition of binding agents to the receiver compartment is usually done to ensure that sink conditions are maintained in the assay. This may at first be counter-intuitive because in those conditions the amount of solute accumulated in the acceptor compartment increases. How does the inclusion of BSA in the assay improve the sink conditions? Assuming the following equilibrium:

Scheme 1 $$\mathrm{Donor} \underset{\boldsymbol{k_b}}{\overset{\boldsymbol{k_f}}{\rightleftharpoons}} \mathrm{Receiver}$$

Where k_f and k_b are the rate constants of the forward and back direction, respectively. Having sink conditions implies that the rate of the back direction has to be much lower than that of the forward direction. Therefore, the concentration of unbound solute in the receiver compartment has to be much smaller than that in the donor, as flow is proportional to the concentration of unbound solute. The addition of BSA to the receiver compartment creates an additional sink condition by imposing the following:

Equation 6 $$[NBD-C4]_U^R \ll [NBD-C4]_T^D$$

The reduction of the back flux of NBD-C4, compared to the assay without BSA, is dependent on the affinity of the solute for BSA.

At the sampling time point, the total concentration of NBD-C4 in the receiver was 2.34 ± 0.04 % of the donor concentration. Although the total concentration in the receiver compartment has increased (as compared with that in the absence of BSA), the concentration of unbound solute (0.25 %) is much smaller, this guaranties that sink conditions are maintained throughout the assay.

3.2.3 Effect of BSA in the donor and receiver compartment

The transport of NBD-C4 was also studied in the presence of BSA in both donor and receiver compartments. The cumulative amount of NBD-C4 transported across the monolayer in function of time are shown in **Figure 19**. The recovery of NBD-C4 was 97 ± 6 % at the end time point.

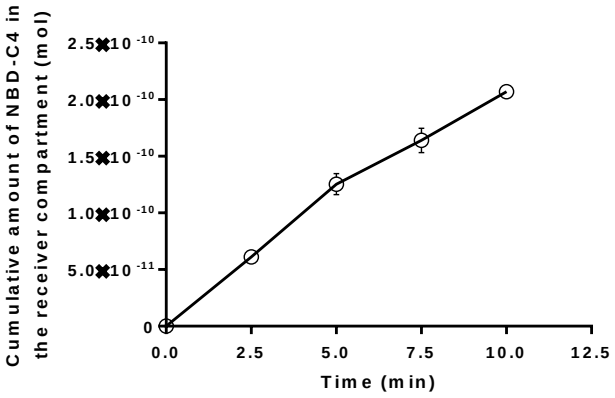

Figure 19 – Cumulative amount of NBD-C4 transported in the A-B direction with BSA in donor and receiver compartments. The results are the mean ± SD of three experiments

The binding of NBD-C4 to the BSA in the donor compartment will decrease the amount of NBD-C4 in the aqueous medium and therefore available to permeate. As a consequence, the P_{app} is expected to decrease under this condition. The P_{app} was calculated considering only the two initial time points (3.2 ± 0.3 x 10^{-5} cm s^{-1}) and all sampling time points (2.7 ± 0.2 x 10^{-5} cm s^{-1}). The P_{app} measured was 3.2 ± 0.3 x 10^{-5} cm s^{-1}, which is much smaller than that obtained with BSA in the receiver compartment only (1.5 x 10^{-4} cm s^{-1}), as expected. To do a quantitative comparison of the transport rates in both conditions it is necessary to account for the unbound fraction of NBD-C4 and recalculate the P_{app} value. The concentration of unbound NBD-C4 at the beginning of the experiment was calculated using the equilibrium constant for binding to BSA (K_B), according to the following equation:

Equation 7
$$\frac{[NBD-C4]_W}{[NBD-C4]_T} = \frac{1}{1+K_B\,[BSA]}$$

Where $[NBD\text{-}C4]_W$ represents the concentration of the amphiphile in the aqueous medium, $[NBD\text{-}C4]_T$ the total concentration in the donor compartment and [BSA] the concentration of BSA in the system. The value of K_B was presented in **Table 1.**.

The concentration of unbound NBD-C4, which is available to permeate was 11 % of the total NBD-C4 added to the donor side at the beginning of the experiment. Thus, considering only the concentration of free NBD-C4 as driving force in Eq. 2, it is expected that the P_{app} will decrease to 11 % of that obtained with the inclusion of BSA in the receiver compartment only. This leads to a value of 1.5 x 10^{-5} cm s^{-1}. Interestingly, this is not the value that was obtained. The obtained P_{app} value (3.2 ± 0.3 x 10^{-5} cm s^{-1}) was higher than the value expected when only the unbound concentration of NBD-C4 is considered. What may be causing this difference?

As shown in the previous section, our Caco-2 monolayer was not fully confluent and does not have well-defined tight junctions. Thus, the first reason that could explain the observed difference is if paracellular permeability is significant. In that case, two routes are possible for the paracellular pathway, through the spaces without cells or through the poorly cohesive tight junctions. While only unbound NBD-C4 may permeate through the cells (transcellular route), NBD-C4 bound to BSA (NBD-C4_BSA) may permeate freely through the filter pores (with a diameter of 0.4 μm). If the permeability of NBD-C4_BSA is not negligible, it would affect the P_{app} measured. Thus, how can the permeability of NBD-C4_BSA be known? The permeability across the filter alone (P_f), in the absence of cells can be used to calculate the permeability through the spaces without cells.

The P_f was calculated in the same way as P_{app}, Eq. 2. The values obtained for the three distinct experimental conditions are presented in **Table 5**. The P_f (NBD-C4_BSA) was only slight lower than the P_f in the absence of BSA. In the presence of 4% BSA in the receiver, we should have observed the P_f of the unbound NBD-C4 and thus, the BSA should have no significant effect on the P_f. However, the value obtained for the P_f was lower compared to the P_f in the absence of BSA. This may be due to flow of BSA from the receiver to the donor compartment. The BSA flow counterbalance the NBD flow drive by the concentration gradient and a lower P_f is obtained. From this, we can anticipate problems in the utilization of BSA only in one side of the monolayer, at least when the cell monolayer is not totally confluent.

Table 5 – Permeability of NBD-C4 across the filter support in the absence and presence of BSA.

P_f x 10^{-5} cm s^{-1}		
no BSA	**4 % BSA receiver**	**4 % BSA donor&receiver**
12.4 ± 1.2	8.2 ± 0.2	7.9 ± 0.3

The results are the mean ± SD of two experiments.

The paracellular permeability of the NBD-C4_BSA can also occur between the cells poorly bonded by the tight junctions. We can assess this permeability calculating the permeability across the cell monolayer only (P_c). The (P_c) was calculated according to Eq 5 and the results are presented in **Table 6**, for the three conditions tested. The decrease observed in the permeability coefficient due to the inclusion of BSA in both the donor and receiver compartment is now closer to the expected value (it is 17 % of that obtained in the absence of BSA). However, a quantitative comparison cannot be done, because the fraction of NBD-C4 that passes through the cells or through the spaces without cells is not known.

Table 6 – Permeability of NBD-C4 across the cell monolayer in in the absence and presence of BSA.

P_c x 10^{-5} cm s^{-1}		
no BSA	**4 % BSA receiver**	**4 % BSA donor&receiver**
31.1	< Ø	5.4

When P_c is calculated for the condition where BSA is added in the receiver compartment only, an impossible value is obtained. The value obtained for P_f was lower than the observed P_{app} leading to a negative value for the calculated P_c. This indicates that the flow of NBD-C4 in the direction A (with NBD-C4, no BSA) to B (no NBD-C4, with BSA) is smaller in the absence of the cell monolayer than in its presence. This unexpected result is due to the flow of BSA from the receiver into the donor compartment, which counterbalance the flow of unbound NBD-C4 from the donor to the receiver compartment. Certainly, this BSA flow is more significant in the absence of cells, but it may also occur to some extent if the cell monolayer is not fully confluent. From this result we conclude that the use of distinct transport media in the donor and receiver compartment should be avoided.

The second possible reason, that could explain the less than expected decrease in the P_{app} values due to the presence of BSA, is the day at which the experiments were performed. The assays in the absence of BSA were performed on day 22 after cell seeding in the inserts, while those in the presence of BSA in both compartments were performed on day 28. Since the assays were performed in different days, variations in the properties of the cell monolayer will affect the results obtained (see section 3.1.1.1).

From day 22 to day 28, the cell monolayer become tighter, showing higher values of TEER and a smaller LY permeation (**Figure 10**). This effect is contrary to the results that we intended to explain. In addition, the P_{app} of NBD-C4 does not vary in a systematic way on the different days, indicating that while this may be affecting the results obtained, it is not the major factor.

Nevertheless, one possible approach is to correct the permeability for the effect of the day. This was done by dividing the P_{app} of NBD-C4 by the P_{app} of the reference compound (LY) at the different experiment days. This treatment of the experimental results leads to a ratio of 40, 125 and 72 for permeability of NBD-C4 relative to that of LY on days 22, 25 and 28, respectively.

This correction indicates an increase in the P_{app} of NBD-C4 relatively to the P_{app} of LY. Certainly, a quantitative analysis is not possible because there are several effects at play. However, it is in fact expected that the permeability of LY is more significantly affected by the cell monolayer growth day. This is because the paracellular route (that followed by LY) will be affected to a larger extent than the transcellular route (that of NBD-C4).

3.2.3 Transport in B-A direction

Generally, the transport studies in the Caco-2 model are performed in both directions across the cell monolayer. The ratio between the two permeability coefficients, is used as evidence for the involvement of an active transport process. If transport in the A-B direction is faster than in the B-A direction, active transport in favor of the concentration gradient is occurring, while the opposite is evidence for the activity of efflux transporters such as P-glycoprotein.

Firstly, the transport of NBD-C4 across the Caco-2 cells was performed in the B-A direction without BSA. The cumulative amount of NBD-C4 transported as function of time is shown in **Figure 20**. The amount transported increases linearly in time with the exception of the first sampling interval where a significantly smaller amount of NBD-C4 was transported. The recovery was 98 ± 0.2 %, which is similar to that obtained in the other assays.

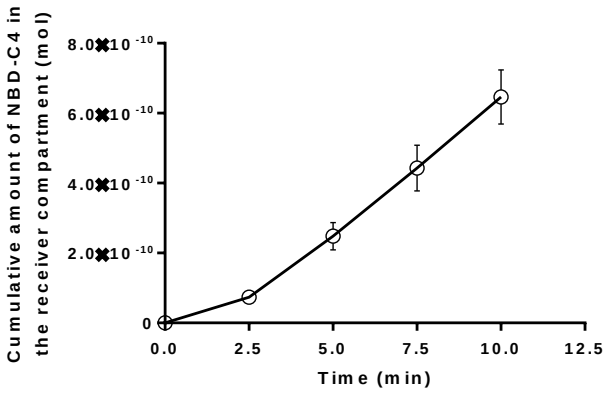

Figure 20 – Cumulative amount of NBD-C4 transported in the B-A direction without BSA. The results are the mean ± SD of six experiments.

Considering only the sampling times after 2.5 min, the P_{app} of NBD-C4 is $9.2 \pm 0.7 \times 10^{-5}$ cm s^{-1} (n = 6) in the B-A direction. This is not significantly different ($p < 0.01$) than the results obtained in the A-B direction ($8.8 \pm 0.4 \times 10^{-5}$ cm s^{-1}).

This results suggests that one of the following two situations is occurring: i) there is no significant by P-gp or ii) the passive permeation of NBD-C4 is too fast to compete with efflux by P-gp. In the former situation, the transporter would be actively transporting NBD-C4 from the inner leaflet of the apical membrane into the donor compartment, but NBD-C4 would quickly return to the membrane and translocate into the inner leaflet, almost totally overcoming the transport by P-glycoprotein. The distinction between the two possibilities may be done *via* a decrease in the rate of passive transport, namely by decreasing the fraction of NBD-C4 available for transport due to the presence of BSA in the transport media.

The cumulative amount of NBD-C4 transported across the cell monolayer in the presence of 4 % of BSA is plotted as function of time in **Figure 21**. A similar behavior was observed for the amount of NBD-C4 transported over time (with a somewhat smaller transport during the first incubation interval). The calculated P_{app} values are reported in **Table 7**.

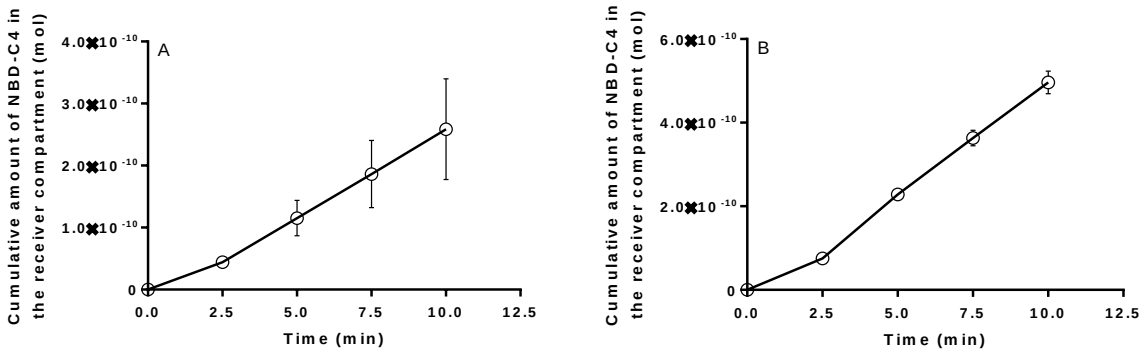

Figure 21 – Cumulative amount of NBD-C4 transported in the A-B direction with BSA. A) BSA was applied in the receiver compartment. B) BSA was added in the donor and receiver compartments. The results are the mean ± SD of three experiments each.

The addition of 4 % BSA to the receiver compartment only, decreased the value of P_{app} relatively to P_{app} without BSA. This result is contrary of what is expected, since the presence of BSA will decrease the rate of backflow of NBD-C4 and therefore should lead to an increase in the measured P_{app}. Again, the inclusion of BSA only in the receiver side of the monolayer leads to artifacts as observed and discussed before for the transport in the A-B direction. In this case, the solution containing BSA is in the compartment above the filter insert containing the cell monolayer. This may lead to a more significant transfer of BSA (in the direction opposite to the flow of NBD-C4) which decreases the overall transport of NBD-C4 observed.

Table 7 – Apparent permeability of NBD-C4 in B-A direction.

P_{app} x 10^{-5} cm s-1		
no BSA	**4 % BSA receiver**	**4 % BSA donor&receiver**
9.2 ± 0.7	2.9 ± 0.9	5.9 ± 0.4

The results are the mean ± SD of n ≥ 3 experiments.

The addition of BSA to the donor compartment decreases the amount of NBD-C4 available to interact with the cell monolayer, leading to a smaller rate of passive permeation.

A significant difference was observed between the P_{app} in the B-A (5.9 ± 0.4 x 10^{-5} cm s^{-1}) and in the A-B direction (3.2 ± 0.3 x 10^{-5} cm s^{-1}) when BSA was present in both the donor and acceptor compartments. The value of P_{app} in the B-A direction is higher, suggesting that NBD-C4 is being transported by P-gp. In fact, there is additional evidence that the NBD-C4 is a substrate of P-gp. This solute stimulates the ATPase

activity of P-gp and competes with the IAAP ([^{125}I] iodoarylazidoprozosin) for the binding to P-gp (results not published, provided by Maria Joao Moreno).

3.3 Transport of NBD-C4 across an *in vitro* BBB model

After 6 days of co-culture with pericytes, the BBB phenotype is induced in the ECs (endothelial cells) (42). Taking into account previous work (42), the generated *in vitro* BBB model with a single monolayer of ECs should be well characterized regarding the morphology, functional tightness and expression of BBB markers.

3.3.1 Characterization and evaluation of the CD34$^+$-ECs monolayer

The integrity and functional tightness of the ECs monolayer was firstly evaluated by measuring the TEER. Then, the paracellular permeability of the ECs monolayer was assessed by performing permeability studies with the LY marker.

After 6 days of co-culture with pericytes, the TEER of the differentiated ECs monolayer was measured in EGM-2 (**Figure 22**). The CD34$^+$-ECs monolayer exhibited a TEER value of 164 ± 7 Ω. cm^2 (n = 6) at 37 º C. The resistance of the Matrigel-coated inserts (119 ± 6 Ω. cm^2 (n = 4)) was subtracted from the resistance obtained in the presence of the endothelial cells. This results in a TEER value of 46 ± 1 Ω. cm^2 (n = 6) for the resistance of the monolayer.

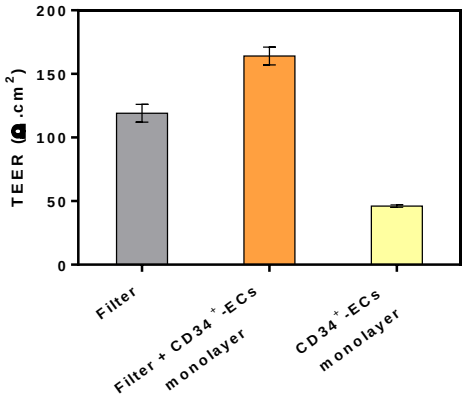

Figure 22 – Evaluation of TEER of the co-culture CD34$^+$-ECs monolayer: TEER measurements of the Matrigel-coated filter (grey, n = 4), CD34$^+$-ECs monolayers in the filter support (orange, n = 6) and CD34$^+$-ECs monolayer (yellow, n = 6) measured at day 7 in culture.

The permeability results from the *in vitro* BBB models are usually presented as endothelial permeability (P_e). The P_e value corresponds to the effective permeability coefficient through the cell monolayer and therefore is the equivalent of P_c used in the Caco-2 model. Thus, the P_e can be calculated according to Eq. 5.

The transport of LY across the $CD34^+$-ECs monolayer was performed after the day 6 in co-culture and conducted in EGM-2 media over 1 hour. The mean P_e of LY obtained was $0.66 \pm 0.27 \times 10^{-3}$ cm/min.

The values measured both for TEER and P_e of LY are in concordance with those obtained during the development of this BBB model (42). Furthermore, the resistance and paracellular permeability values for the co-cultured $CD34^+$-ECs monolayer were similar to the values reported in other *in vitro* BBB models (42).

The nuclei and expression of tight junctions of the 6 days differentiated $CD34^+$-ECs monolayers were analyzed by confocal microscopy (**Figure 23**). Images of the $CD34^+$-ECs showed a uniform monolayer, with cells fully confluent in the filter support. Accordingly, the staining of the tight junction showed a continuous and regular expression pattern of Z0 -1 at cells borders.

The results indicated the formation of a regular monolayer of ECs with well-developed tight junction, after the day 6 in co-culture.

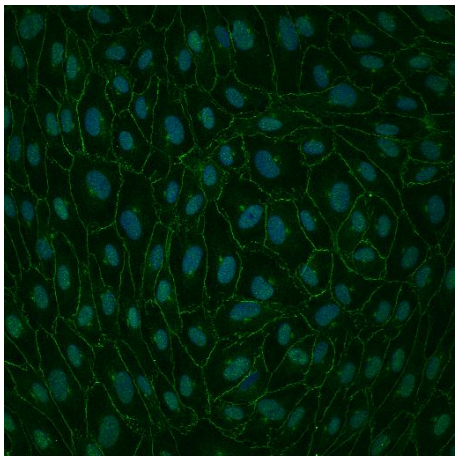

Figure 23 – $CD34^+$-ECs monolayer stained for tight junctions (Z0-1). Images were acquired with a 40 x in immersion oil objective. Expression of Z0-1 (green) marker was obtained by immunofluorescence. The nuclei (blue) were stained with Hoescht.

An important feature of an *in vitro* BBB model is the functional tightness, since this is responsible for the barrier function of the *in vivo* BBB (9). The tight junctions contribute to this tightness by causing a restriction in the paracellular pathway of hydrophilic

solutes. Thus, in an *in vitro* BBB model it is expected to found high TEER values and very low paracellular permeability (i.e: LY permeability).

However, the TEER value of the generated *in vitro* BBB model is significantly smaller than that obtained using the Caco-2 model. It should be noted that the value of TEER is affected by the composition of the transport media, which is different in both assays. A better evaluation is provided by the permeability of paracellular markers such as LY.

The measured P_{app} for LY was 7.66 x 10^{-6} cm/s.

When compared with the results obtained with the Caco-2 model, the results obtained with this BBB model indicate a more permeable barrier, both in terms of LY permeability and TEER values. This comparison cannot be direct since the Caco-2 cells display different morphology and gene expression as well as different cell–cell junctions. Nevertheless, if the BBB model is tighter a smaller permeability of LY and higher TEER values were expected when compared with an epithelial *in vitro* model.

This is a disturbing result, although in agreement with data in the literature that must be addressed and understood in the future.

3.3.2 Effect of the experimental conditions on CD34^{+}-ECs monolayer viability and integrity

Initially, the cytotoxicity of the CD34^{+}-ECs was evaluated for the incubation with media for 2h or with media contained NBD-C4 for 1 h followed by incubation with media for additional hour at 37°C with stirring (35 rpm with an orbit 1.9 mm) (**Figure 24A**). The results show a decrease in cell viability both when incubated with EBM-2 alone (not supplemented medium) or with EBM-2 containing NBD-C4. This data suggests that that NBD-C4 is not toxic to the cells, and also that the cells cannot be maintained for 2h without the supplemented medium. Thus, we performed another identical experiment but where the cells were incubated for 1h with EBM-2 or with EBM-2 containing NBD C4 (**Figure 24B**). The results showed that NBD-C4 is not toxic to the CD34^{+}-ECs after 1 h of incubation in EBM-2. Also, the experimental conditions, including the stirring rate, do not affect cell viability.

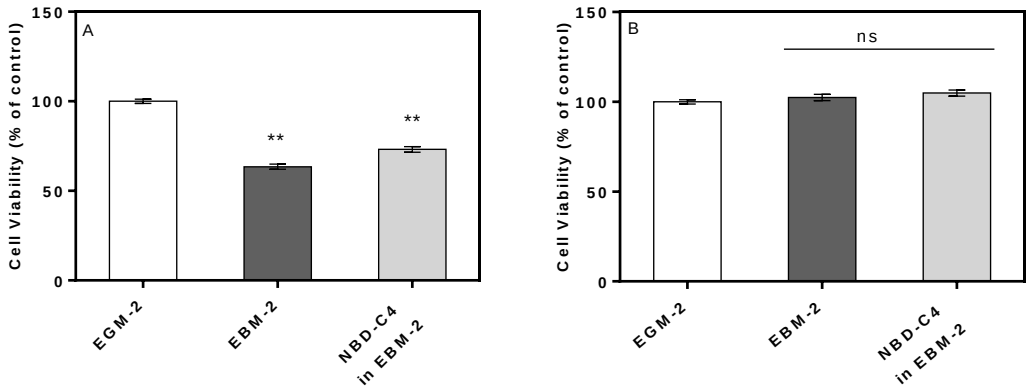

Figure 24 – Effect of the experimental conditions in CD34$^+$-ECs viability: Cell viability was assessed A) after 2h of incubation (1h with NBD-C4 plus 1h in EBM-2) and B) after 1h of incubation with the compound. The supplement medium EGM-2 was used as control. Results are mean ± SD of three replicates. Significant difference from the control ($p < 0.01$).

We have also evaluated the effect of the experimental conditions used in the permeability assay on the integrity of the CD34$^+$-ECs monolayer For this, TEER was measured before and after the permeability assay with NBD-C4 (**Figure 25**). The measured TEER value at the end of the experiment was not statistically different from the TEER value before the experiment, although a much higher standard deviation is obtained. This indicates that the sampling method, the time, the compound and the stirring rate were not affecting the monolayer integrity.

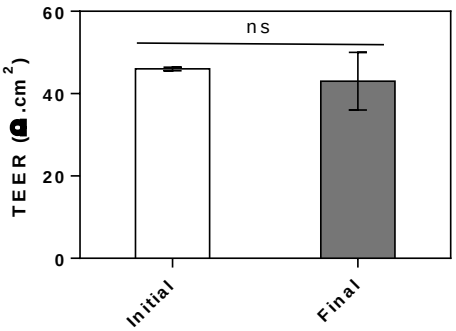

Figure 25 – Effect of the experimental conditions on CD34$^+$ -ECs monolayer integrity. Evaluation of TEER before and after the permeability assays of NBD-C4 at day 7. Results are mean ± SD of six experiments each.

3.3.3 Transport of NBD-C4 in the *in vitro* BBB model

The permeation of NBD-C4 across the $CD34^+$-ECs monolayer was measured in the A-B and B-A directions. The cumulative amount of NBD-C4 transported into the receiver compartment as a function of time is presented in **Figure 26.**

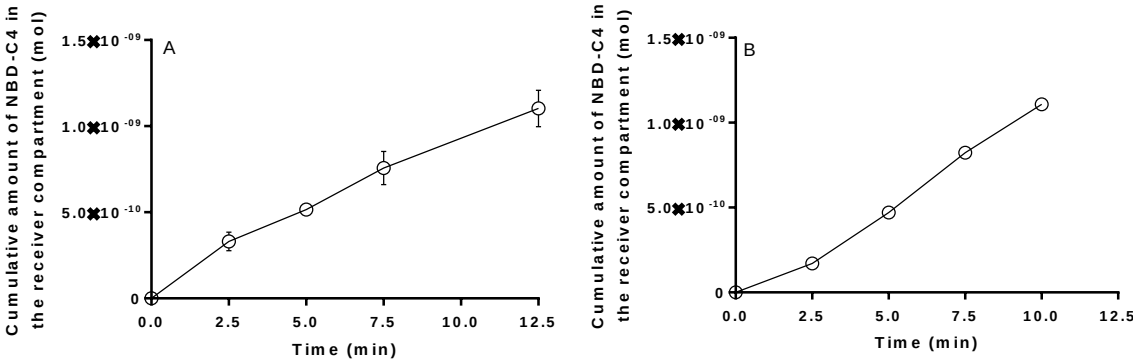

Figure 26 – Cumulative amount of NBD-C4 transported across the $CD34^+$ -ECs monolayer. The permeability was measured A) in the A-B direction and B) in the B-A direction. The results are the mean ± SD of three experiments each.

It is observed that in the B-A direction less amount of NBD-C4 was transported in the first sampling interval ((as observed before for the Caco-2 model). Indeed, 0.9 ± 0.1 % of the initial amount in the donor side was transported across the cell monolayer during the first 2.5 min incubation. Contrarily, 7.8 ± 1.3 % of NBD-C4 added to the donor was accumulated in the receiver side when transport was in the A-B direction. The recovery of NBD-C4 at the end point of the assay was 108 ± 5 % and 98 ± 11 % for A-B and B-A direction, respectively. This indicates no cellular retention or adsorption to the plastic surfaces of the Transwell.

The P_{app} values were calculated using the Eq. 2 and are presented in **Figure 27**. The P_{app} in the A-B direction (1.42 ± 0.15 x 10^{-4} cm/s) was not significantly different ($p < 0.01$) from the P_{app} in the B-A direction (1.10 ± 0.25 x 10^{-4} cm/s). The NBD-C4 was rapidly transported across the CD34+ -ECs monolayer in both directions. This data may suggest that there is no efflux transport of NBD-C4 to the apical side of the monolayer. However, as discussed in the previous section, this could result from the fast passive permeation of NBD-C4 with which the efflux transporters could not compete.

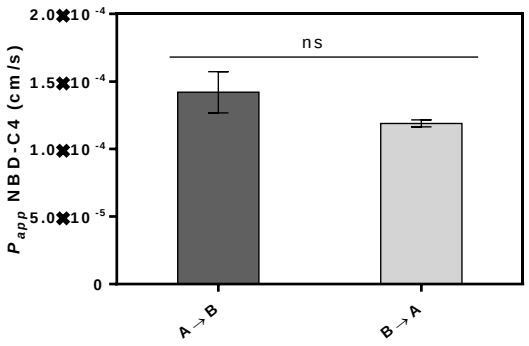

Figure 27 –Apparent permeability of NBD-C4 across the CD34+-ECs monolayer. The A to B was not significantly different ($p < 0.01$) from B to A. The results are the mean ± SD of three experiments.

When the results of NBD-C4 permeability in both models are compared one finds a higher permeability rate through the $CD34^{+}$-ECs monolayer. This result is in tandem with the higher permeability coefficient of LY and smaller TEER for the $CD34^{+}$-ECs cell monolayer.

Chapter 4

Conclusion

4.1 General conclusions

Although the Caco-2 model is well-characterized and with detailed protocols available in the literature, its establishment for the first time in a laboratory is not a trivial process. Before new molecules are evaluated, a full characterization in terms of cell morphology and barrier leakiness must be performed.

In this work, we implement the *in vitro* permeability assays using the Caco-2 model for the first time in our laboratory. Although after 21 days in culture the Caco-2 monolayers prepared pass the quality control in terms of TEER (≥ 165 Ω cm^{-2}) (25) the permeability of the paracellular marker LY is too high. This indicates that the Caco-2 monolayer obtained by us is not as tight as that characterized in the literature when following the same protocol (25). However, it is observed an improvement in barrier properties of the cell monolayer (both in terms of TEER and LY permeability) when the time of differentiation is increased from 21 to 28 days. On day 28 both criteria are fulfilled by the cell monolayer prepared in this work. It should be noted that the reference protocol followed (25) refers to cells at passage 95 to 105, while in this work passages 50 to 60 were used. This may be the reason for the contradictory results in terms of both criteria. That means, a confluent cell monolayer being formed (low TEER) but with tight junctions not properly developed (high paracellular permeation of small solutes). To further elucidate on this subject, cells on passage 95 to 105will be used in future work.

The confocal microscopy characterization reveals that the Caco-2 cell monolayer is not fully confluent. This is evident in the observation that some cells are still dividing. According to literature, cell differentiation only starts after confluence is achieved.(26). Therefore, our cell monolayer is not expected to be fully differentiated with well-developed tight junctions. This would lead to a higher paracellular permeability, as observed for LY.

In conclusion, although the Caco-2 cell monolayers shows to be reproducible, it is not fully comparable with that developed in reference protocols available in the literature. It must be further optimized, see future perspectives below.

We also found that the stirring rate used in the permeability assays is affecting the cell monolayer TEER, and thereofe, the monolayer integrity. The stirring used is however the minimum vale reported in the literature. From those results we may only speculate that non-fully differentiated cells are more sensitive to stirring. We should note however that this control is very rarely performed (or at least shown).

The permeability assays with the chosen compound, NBD-C4 were very conclusive in some important aspects. One of them is that it is problematic to use BSA only in one of

the compartments. This is particularly relevant when the Caco-2 cell monolayer is not full confluent and tight. Under this condition, the apparent permeability coefficient of NBD-C4 is affected by the paracellular permeability (through the spaces without cells or through the poorly cohesive tight junctions) of the NBD-C4 bound to BSA. In addition, the different media on both sides of the filter may lead to solution flow leading to unpredictable effects of the observed solute transport. It is highlighted that a quantitative analysis of the effect of BSA on the measured P_{app} is not possible under this conditions.

When BSA is added to the transport media on both sides of the cell monolayer, the effect on solute permeability is qualitatively the expected one (decrease in Papp due to a smaller amount of solute available to permeate). The results obtained cannot yet be interpreted quantitatively, possibly due to a significant contribution of transport through the paracellular pathway.

Overall, this results contributes to a better understanding of the permeability experiments using the Caco-2 model, while demonstrates that not having an optimal model could lead to artificial P_{app} values.

We apply the same protocol to perform permeability assays in a recently developed *in vitro* BBB model. Even though the BBB model exhibits a confluent monolayer of ECs with a regular network of tight junction between the cells, the TEER values obtained are low and the LY permeability is high. It should be stressed that the values obtained in this work are in full agreement with those reported in the literature for this model. This was expected as the work was done in the same laboratory were the model was developed. The doubt persists on whether an *in vitro* BBB model should present a higher paracellular permeability than an intestinal model.

The NBD-C4 is found to have a fast permeation rate in the both cell models, in agreement with the predictions from its interaction with membrane model systems (21, 76).

4.2 Future prospects

The results obtained in this work highlight the importance of having a fully-confluent cell monolayer. Our first approach towards this goal is to follow the same protocol but using cells with a higher passage number (eg. 95-105 as indicated in reference (25)). During the present work this was not possible, because the cells were acquired in passage 44 (the latest available commercially), and it takes over 6 months to reach passage 95. The work was therefore performed with cells on passage 50 which was also indicated in the protocol being followed. In the meantime, cells on a higher passage number were being obtained, and only preliminary experiments could be undertaken.

If a fully confluent cell monolayer with full differentiation at day 21 after seeding is still not obtained from cells with the high passage numbers, some additional changes in the protocol may be attempted. First, the number of cell used for seeding will be increased. An additional modification may be the time of media change after seeding. With those changes we expect to have a higher number of cells adherent to the filter, leading to confluence being achieved earlier, and hopefully to full differentiation at day 21 after seeding.

The permeability assays through Caco-2 cell monolayers is a very expensive methodology, both in terms of material, time and human resources. Attempts to decrease the cost of this methodology have been focused only on the decrease of the time required for confluence and differentiation (31). It would however be very convenient if the confluent and differentiated cell monolayer could be used for several permeation experiments. Our preliminary results indicate that when using cells on passage 50, the cell monolayer is not stable enough to allow its use in distinct days after seeding. We anticipate that this could be possible when a fully confluent and differentiated cell monolayer is obtained at day 21. To validate the re-use of the cell monolayer it is necessary to perform permeability assays using a solute that permeates through the paracellular and another permeating through the transcellular pathway. An experiment with unused cell monolayers at the distinct days will give information regarding the monolayer stability. If the cell monolayer is stable, repeated permeability experiments will be performed using the same cell monolayer. Because the permeability assays are performed in media without supplements, after each permeability assay the cell monolayer must be maintained in grow media to reestablish its properties. The preliminary data obtained in this work suggests that two day incubation with media is enough between permeability assays.

The use of distinct transport media in the donor and acceptor compartments is commonly found in the literature.(50, 51, 74) The results obtained in this work strongly discourage this procedure. It is however very important to evaluate if this problem persists when a fully confluent and differentiated cell monolayer is used.

In the *in vitro* BBB model used, the filters inserts where coated with Matrigel while Caco-2 cells are grown directly on the filter. The matrix is used to improve the adherence of the cells to the filter. The effect of the coating on solute permeation is however not well characterized. Only after this evaluation, it is possible to compare the results obtained with the Caco-2 model with those using the BBB model. The effect of Matrigel coating will be tested seeding the Caco-2 cells on coated filters.

Chapter 5

Bibliography

1. Stenberg, P., U. Norinder, K. Luthman, and P. Artursson. 2001. Experimental and computational screening models for the prediction of intestinal drug absorption. J Med Chem 44:1927.
2. Stenberg, P., K. Luthman, and P. Artursson. 2000. Virtual screening of intestinal drug permeability. Journal of Controlled Release 65:231-243.
3. Gary, W. C., M. R. David, A. M. John, H. William, and Y. Zhengyin. 2001. The New Pre-Preclinical Paradigm: Compound Optimization in Early and Late Phase Drug Discovery. Current Topics in Medicinal Chemistry 1:353-366.
4. Tsaioun, K., M. Bottlaender, A. Mabondzo, and F. the Alzheimer's Drug Discovery. 2009. ADDME – Avoiding Drug Development Mistakes Early: central nervous system drug discovery perspective. BMC Neurology 9:S1-S1.
5. DiMasi, J. A., H. G. Grabowski, and R. W. Hansen. 2016. Innovation in the pharmaceutical industry: New estimates of R&D costs. Journal of Health Economics 47:20-33.
6. Sugano, K., M. Kansy, P. Artursson, A. Avdeef, S. Bendels, L. Di, G. F. Ecker, B. Faller, H. Fischer, G. Gerebtzoff, H. Lennernaes, and F. Senner. 2010. Coexistence of passive and carrier-mediated processes in drug transport. Nature Reviews Drug Discovery 9:597.
7. Quignot, N. 2013. Modeling bioavailability to organs protected by biological barriers. In Silico Pharmacology 1:8.
8. Ismael, J. H. 2001. Assessing the Absorption of New Pharmaceuticals. Current Topics in Medicinal Chemistry 1:385-401.
9. Abbott, N. J., A. A. K. Patabendige, D. E. M. Dolman, S. R. Yusof, and D. J. Begley. 2010. Structure and function of the blood–brain barrier. Neurobiology of Disease 37:13-25.
10. Cecchelli, R., V. Berezowski, S. Lundquist, M. Culot, M. Renftel, M.-P. Dehouck, and L. Fenart. 2007. Modelling of the blood–brain barrier in drug discovery and development. Nature Reviews Drug Discovery 6:650.
11. Sarmento, B., F. Andrade, S. B. da Silva, F. Rodrigues, J. das Neves, and D. Ferreira. 2012. Cell-based in vitro models for predicting drug permeability. Expert Opinion on Drug Metabolism & Toxicology 8:607-621.
12. van Breemen, R. B., and Y. Li. 2005. Caco-2 cell permeability assays to measure drug absorption. Expert Opinion on Drug Metabolism & Toxicology 1:175-185.
13. Bohets, H., P. Annaert, G. Mannens, K. Anciaux, P. Verboven, W. Meuldermans, and K. Lavrijsen. 2001. Strategies for absorption screening in drug discovery and development. Current topics in medicinal chemistry 1:367-383.
14. He, Y., Y. Yao, S. E. Tsirka, and Y. Cao. 2014. Cell-Culture Models of the Blood–Brain Barrier. Stroke; a journal of cerebral circulation 45:2514-2526.
15. Helms, H. C., N. J. Abbott, M. Burek, R. Cecchelli, P.-O. Couraud, M. A. Deli, C. Förster, H. J. Galla, I. A. Romero, E. V. Shusta, M. J. Stebbins, E. Vandenhaute, B. Weksler, and B. Brodin. 2016. In vitro models of the blood–brain barrier: An overview of commonly used brain endothelial cell culture models and guidelines for their use. Journal of Cerebral Blood Flow & Metabolism 36:862-890.
16. Tavelin, S., J. Gråsjö, J. Taipalensuu, G. Ocklind, and P. Artursson. 2002. Applications of Epithelial Cell Culture in Studies of Drug Transport. In Epithelial Cell Culture Protocols. C. Wise, editor. Humana Press, Totowa, NJ. 233-272.
17. Flaten, G. E., A. B. Dhanikula, K. Luthman, and M. Brandl. 2006. Drug permeability across a phospholipid vesicle based barrier: A novel approach for studying passive diffusion. european journal of pharmaceutical sciences 27:80-90.
18. Clark, D. E., and S. D. Pickett. 2000. Computational methods for the prediction of 'drug-likeness'. Drug discovery today 5:49-58.
19. Kitchen, D. B., H. Decornez, J. R. Furr, and J. Bajorath. 2004. Docking and scoring in virtual screening for drug discovery: methods and applications. Nature reviews Drug discovery 3:935.

20. Sun, H., and K. S. Pang. 2008. Permeability, transport, and metabolism of solutes in Caco-2 cell monolayers: a theoretical study. Drug Metabolism and Disposition 36:102-123.
21. Filipe, H., A. Salvador, J. Silvestre, W. Vaz, and M. Moreno. 2014. Beyond Overton's rule: quantitative modeling of passive permeation through tight cell monolayers. Molecular pharmaceutics 11:3696-3706.
22. Balimane, P. V., S. Chong, and R. A. Morrison. 2000. Current methodologies used for evaluation of intestinal permeability and absorption. J. Pharmacol. Toxicol. Methods 44:301-312.
23. Hidalgo, I. J., T. J. Raub, and R. T. Borchardt. 1989. Characterization of the human colon carcinoma cell line (Caco-2) as a model system for intestinal epithelial permeability. Gastroenterology 96:736-749.
24. Sun, H., E. C. Y. Chow, S. Liu, Y. Du, and K. S. Pang. 2008. The Caco-2 cell monolayer: usefulness and limitations. Expert Opinion on Drug Metabolism & Toxicology 4:395-411.
25. Hubatsch, I., E. G. E. Ragnarsson, and P. Artursson. 2007. Determination of drug permeability and prediction of drug absorption in Caco-2 monolayers. Nature Protocols 2:2111-2119.
26. Lea, T. 2015. Caco-2 Cell Line. In The Impact of Food Bioactives on Health: in vitro and ex vivo models. K. Verhoeckx, P. Cotter, I. López-Expósito, C. Kleiveland, T. Lea, A. Mackie, T. Requena, D. Swiatecka, and H. Wichers, editors. Springer International Publishing, Cham. 103-111.
27. Artursson, P., and J. Karlsson. 1991. Correlation between oral drug absorption in humans and apparent drug permeability coefficients in human intestinal epithelial (Caco-2) cells. Biochemical and Biophysical Research Communications 175:880-885.
28. Alsenz, J., H. Steffen, and R. Alex. 1998. Active apical secretory efflux of the HIV protease inhibitors saquinavir and ritonavir in Caco-2 cell monolayers. Pharmaceutical research 15:423-428.
29. Anderle, P., E. Niederer, W. Rubas, C. Hilgendorf, H. Spahn-Langguth, H. Wunderli-Allenspach, H. P. Merkle, and P. Langguth. 1998. P-glycoprotein (P-gp) mediated efflux in Caco-2 cell monolayers: The influence of culturing conditions and drug exposure on P-gp expression levels. Journal of pharmaceutical sciences 87:757-762.
30. Artursson, P., K. Palm, and K. Luthman. 2011 Caco-2 monolayers in experimental and theoretical predictions of drug transport. Advanced Drug Delivery Reviews 46:27-43.
31. Yamashita, S., K. Konishi, Y. Yamazaki, Y. Taki, T. Sakane, H. Sezaki, and Y. Furuyama. 2002. New and better protocols for a short-term Caco-2 cell culture system. Journal of Pharmaceutical Sciences 91:669-679.
32. Pontier, C., J. Pachot, R. Botham, B. Lenfant, and P. Arnaud. 2001. HT29-MTX and Caco-2/TC7 monolayers as predictive models for human intestinal absorption: Role of the mucus layer. Journal of pharmaceutical sciences 90:1608-1619.
33. Abbott, N. J., L. Rönnbäck, and E. Hansson. 2006. Astrocyte–endothelial interactions at the blood–brain barrier. Nature Reviews Neuroscience 7:41.
34. Abbott, N. J. 2002. Astrocyte–endothelial interactions and blood–brain barrier permeability. Journal of Anatomy 200:629-638.
35. Cardoso, F. L., D. Brites, and M. A. Brito. 2010. Looking at the blood–brain barrier: Molecular anatomy and possible investigation approaches. Brain Research Reviews 64:328-363.
36. Naik, P., and L. Cucullo. 2012. In Vitro Blood-Brain Barrier Models: Current and Perspective Technologies. Journal of Pharmaceutical Sciences 101:1337-1354.

37. Gumbleton, M., and K. L. Audus. 2001. Progress and limitations in the use of *in vitro* cell cultures to serve as a permeability screen for the blood-brain barrier. Journal of Pharmaceutical Sciences 90:1681-1698.
38. Bernas, M. J., F. L. Cardoso, S. K. Daley, M. E. Weinand, A. R. Campos, A. J. G. Ferreira, J. B. Hoying, M. H. Witte, D. Brites, Y. Persidsky, S. H. Ramirez, and M. A. Brito. 2010. Establishment of primary cultures of human brain microvascular endothelial cells to provide an in vitro cellular model of the blood-brain barrier. Nature Protocols 5:1265.
39. Aday, S., R. Cecchelli, D. Hallier-Vanuxeem, M. P. Dehouck, and L. Ferreira. 2016. Stem Cell-Based Human Blood-Brain Barrier Models for Drug Discovery and Delivery. Trends in Biotechnology 34:382-393.
40. Lippmann, E. S., A. Al-Ahmad, S. P. Palecek, and E. V. Shusta. 2013. Modeling the blood–brain barrier using stem cell sources. Fluids and Barriers of the CNS 10:2.
41. Tóth, A., S. Veszelka, S. Nakagawa, M. Niwa, and M. A Deli. 2011. Patented in vitro blood-brain barrier models in CNS drug discovery. Recent patents on CNS drug discovery 6:107-118.
42. Cecchelli, R., S. Aday, E. Sevin, C. Almeida, M. Culot, L. Dehouck, C. Coisne, B. Engelhardt, M.-P. Dehouck, and L. Ferreira. 2014. A Stable and Reproducible Human Blood-Brain Barrier Model Derived from Hematopoietic Stem Cells. PLOS ONE 9:e99733.
43. Garberg, P., M. Ball, N. Borg, R. Cecchelli, L. Fenart, R. D. Hurst, T. Lindmark, A. Mabondzo, J. E. Nilsson, T. J. Raub, D. Stanimirovic, T. Terasaki, J. O. Öberg, and T. Österberg. 2005. In vitro models for the blood–brain barrier. Toxicology in Vitro 19:299-334.
44. Hellinger, É., S. Veszelka, A. E. Tóth, F. Walter, Á. Kittel, M. L. Bakk, K. Tihanyi, V. Háda, S. Nakagawa, T. Dinh Ha Duy, M. Niwa, M. A. Deli, and M. Vastag. 2012. Comparison of brain capillary endothelial cell-based and epithelial (MDCK-MDR1, Caco-2, and VB-Caco-2) cell-based surrogate blood–brain barrier penetration models. European Journal of Pharmaceutics and Biopharmaceutics 82:340-351.
45. Lundquist, S., M. Renftel, J. Brillault, L. Fenart, R. Cecchelli, and M.-P. Dehouck. 2002. Prediction of drug transport through the blood-brain barrier in vivo: a comparison between two in vitro cell models. Pharmaceutical research 19:976-981.
46. Hakkarainen, J. J., A. J. Jalkanen, T. M. Kääriäinen, P. Keski-Rahkonen, T. Venäläinen, J. Hokkanen, J. Mönkkönen, M. Suhonen, and M. M. Forsberg. 2010. Comparison of in vitro cell models in predicting in vivo brain entry of drugs. International journal of pharmaceutics 402:27-36.
47. Srinivasan, B., A. R. Kolli, M. B. Esch, H. E. Abaci, M. L. Shuler, and J. J. Hickman. 2015. TEER measurement techniques for in vitro barrier model systems. Journal of laboratory automation 20:107-126.
48. Delie, F., and W. Rubas. 1997. A human colonic cell line sharing similarities with enterocytes as a model to examine oral absorption: advantages and limitations of the Caco-2 model. Critical Reviews™ in Therapeutic Drug Carrier Systems 14.
49. Youdim, K. A., A. Avdeef, and N. J. Abbott. 2003. In vitro trans-monolayer permeability calculations: often forgotten assumptions. Drug Discovery Today 8:997-1003.
50. Neuhoff, S., P. Artursson, I. Zamora, and A.-L. Ungell. 2006. Impact of Extracellular Protein Binding on Passive and Active Drug Transport Across Caco-2 Cells. Pharmaceutical Research 23:350-359.
51. Broeders, J. J. W., J. C. H. van Eijkeren, B. J. Blaauboer, and J. L. M. Hermens. 2012. Transport of Chlorpromazine in the Caco-2 Cell Permeability Assay: A Kinetic Study. Chemical Research in Toxicology 25:1442-1451.
52. Karlsson, J., and P. Artursson. 1991. A method for the determination of cellular permeability coefficients and aqueous boundary layer thickness in monolayers of

intestinal epithelial (Caco-2) cells grown in permeable filter chambers. International journal of pharmaceutics 71:55-64.
53. Korjamo, T., A. T. Heikkinen, P. Waltari, and J. Mönkkönen. 2008. The Asymmetry of the Unstirred Water Layer in Permeability Experiments. Pharmaceutical Research 25:1714.
54. Korjamo, T., A. T. Heikkinen, and J. Mönkkönen. 2009. Analysis of unstirred water layer in in vitro permeability experiments. Journal of pharmaceutical sciences 98:4469-4479.
55. Castillo-Garit, J. A., Y. Marrero-Ponce, F. Torrens, and R. García-Domenech. 2008. Estimation of ADME properties in drug discovery: Predicting Caco-2 cell permeability using atom-based stochastic and non-stochastic linear indices. Journal of pharmaceutical sciences 97:1946-1976.
56. Volpe, D. A. 2008. Variability in Caco-2 and MDCK cell-based intestinal permeability assays. Journal of Pharmaceutical Sciences 97:712-725.
57. Briske-Anderson, M. J., J. W. Finley, and S. M. Newman. 1997. The influence of culture time and passage number on the morphological and physiological development of Caco-2 cells. Proceedings of the society for experimental biology and medicine 214:248-257.
58. Bailey, C. A., P. Bryla, and A. W. Malick. 1996. The use of the intestinal epithelial cell culture model, Caco-2, in pharmaceutical development. Advanced Drug Delivery Reviews 22:85-103.
59. Artursson, P., K. Palm, and K. Luthman. 1996. Caco-2 monolayers in experimental and theoretical predictions of drug transport. Advanced Drug Delivery Reviews 22:67-84.
60. Hayeshi, R., C. Hilgendorf, P. Artursson, P. Augustijns, B. Brodin, P. Dehertogh, K. Fisher, L. Fossati, E. Hovenkamp, T. Korjamo, C. Masungi, N. Maubon, R. Mols, A. Müllertz, J. Mönkkönen, C. O'Driscoll, H. M. Oppers-Tiemissen, E. G. E. Ragnarsson, M. Rooseboom, and A.-L. Ungell. 2008. Comparison of drug transporter gene expression and functionality in Caco-2 cells from 10 different laboratories. European Journal of Pharmaceutical Sciences 35:383-396.
61. Oltra-Noguera, D., V. Mangas-Sanjuan, A. Centelles-Sangüesa, I. Gonzalez-Garcia, G. Sanchez-Castaño, M. Gonzalez-Alvarez, V.-G. Casabo, V. Merino, I. Gonzalez-Alvarez, and M. Bermejo. 2015. Variability of permeability estimation from different protocols of subculture and transport experiments in cell monolayers. J. Pharmacol. Toxicol. Methods 71:21-32.
62. Sambuy, Y., I. De Angelis, G. Ranaldi, M. L. Scarino, A. Stammati, and F. Zucco. 2005. The Caco-2 cell line as a model of the intestinal barrier: influence of cell and culture-related factors on Caco-2 cell functional characteristics. Cell Biology and Toxicology 21:1-26.
63. Vachon, P. H., and J.-F. Beaulieu. 1992. Transient mosaic patterns of morphological and functional differentiation in the Caco-2 cell line. Gastroenterology 103:414-423.
64. Meunier, V., M. Bourrie, Y. Berger, and G. Fabre. 1995. The human intestinal epithelial cell line Caco-2; pharmacological and pharmacokinetic applications. Cell biology and toxicology 11:187-194.
65. Lee, J. B., A. Zgair, D. A. Taha, X. Zang, L. Kagan, T. H. Kim, M. G. Kim, H.-y. Yun, P. M. Fischer, and P. Gershkovich. 2017. Quantitative analysis of lab-to-lab variability in Caco-2 permeability assays. European Journal of Pharmaceutics and Biopharmaceutics 114:38-42.
66. Ingels, F. M., and P. F. Augustijns. 2003. Biological, Pharmaceutical, and Analytical Considerations with Respect to the Transport Media Used in the Absorption Screening System, Caco-2. Journal of Pharmaceutical Sciences 92:1545-1558.
67. Neuhoff, S., A.-L. Ungell, I. Zamora, and P. Artursson. 2003. pH-Dependent Bidirectional Transport of Weakly Basic Drugs Across Caco-2 Monolayers: Implications for Drug–Drug Interactions. Pharmaceutical Research 20:1141-1148.

68. Yamashita, S., T. Furubayashi, M. Kataoka, T. Sakane, H. Sezaki, and H. Tokuda. 2000. Optimized conditions for prediction of intestinal drug permeability using Caco-2 cells. European Journal of Pharmaceutical Sciences 10:195-204.
69. Buckley, S. T., S. M. Fischer, G. Fricker, and M. Brandl. 2012. In vitro models to evaluate the permeability of poorly soluble drug entities: Challenges and perspectives. European Journal of Pharmaceutical Sciences 45:235-250.
70. Palmgrén, J. J., J. Mönkkönen, T. Korjamo, A. Hassinen, and S. Auriola. 2006. Drug adsorption to plastic containers and retention of drugs in cultured cells under in vitro conditions. European Journal of Pharmaceutics and Biopharmaceutics 64:369-378.
71. Krishna, G., K.-j. Chen, C.-c. Lin, and A. A. Nomeir. 2001. Permeability of lipophilic compounds in drug discovery using in-vitro human absorption model, Caco-2. International journal of pharmaceutics 222:77-89.
72. Volpe, D. A. 2011. Drug-permeability and transporter assays in Caco-2 and MDCK cell lines. Future Medicinal Chemistry 3:2063-2077.
73. Volpe, D. A. 2010. Application of Method Suitability for Drug Permeability Classification. The AAPS Journal 12:670-678.
74. Aungst, B. J., N. H. Nguyen, J. P. Bulgarelli, and K. Oates-Lenz. 2000. The influence of donor and reservoir additives on Caco-2 permeability and secretory transport of HIV protease inhibitors and other lipophilic compounds. Pharmaceutical Research 17:1175-1180.
75. Cardoso, R. M., P. A. Martins, F. Gomes, S. Doktorovova, W. L. Vaz, and M. J. Moreno. 2011. Chain-length dependence of insertion, desorption, and translocation of a homologous series of 7-nitrobenz-2-oxa-1, 3-diazol-4-yl-labeled aliphatic amines in membranes. The Journal of Physical Chemistry B 115:10098-10108.
76. Cardoso, R., H. Filipe, F. Gomes, N. Moreira, W. Vaz, and M. Moreno. 2010. Chain length effect on the binding of amphiphiles to serum albumin and to POPC bilayers. The Journal of Physical Chemistry B 114:16337-16346.
77. Filipe, H. A. L., D. Bowman, T. Palmeira, R. M. S. Cardoso, L. M. S. Loura, and M. J. Moreno. 2015. Interaction of NBD-labelled fatty amines with liquid-ordered membranes: a combined molecular dynamics simulation and fluorescence spectroscopy study. Physical Chemistry Chemical Physics 17:27534-27547.